ISIJ International, Vol. 30 (1990), No. 12, pp. 1011-1032

Review

Metal/Ceramic Joining

G. ELSSNER and G. PETZOW

Max-Planck-Institut für Metallforschung, Institut für Werkstoffwissenschaft, D-7000 Stuttgart 1, F. R. Germany.

(*Received on May 28,1990; accepted in the final form on June 29, 1990*)

This review article on metal/ceramic joining is subdivided into the description of research activities in the fields of active metal brazing and diffusion bonding published in the last decade. Informations are given on active metal brazing of oxide, nitride, and carbide ceramics and on diffusion bonding of alumina, zirconia, magnesia, silicon nitride, aluminum nitride and silicon carbide ceramics to metals. Ultra high vacuum diffusion bonding and experiments using the model combination Nb/alumina are also regarded. Emphasis is laid on a concise reproduction of experimental data concerning the bonding conditions and the determination of bond strength. The review demonstrates that much effort was devoted to studies on the fromatin of interfacial reaction layers and on the efficiency of interlayers additionally introduced between the ceramic and the metal part to reduce internal stresses caused by thermal expansion misfit of the materials to be bonded.

KEY WORDS: active metal brazing; bond strength; diffusion bonding; interlayer; metal/ceramic joining; reaction layer; ultra high vacuum diffusion bonding.

1. Introduction

New high performance ceramics are both important structural and electrical materials which will be used also in electronic devices and in chemical engineering. However, their technical application depends strongly on the reliability of joining techniques especially to metals and metal alloy components in which ceramic materials have mostly to be incorporated. Amongst the many techniques employed to join ceramics to metals, ranging from fusion welding to mechanical attachment, active metal brazing, and diffusion bonding are generally preferred in modern research and development work. Mainly these methods will guarantee the soundness of metal/ceramic joints under severe environmental conditions as high mechanical stresses, high temperatures, corrosion and chemical attack or combinations of them.

Technological progress in the field of metal/ceramic joining can only be achieved if its scientific background is also investigated. This is an interdisciplinary task in which different fields of materials science must participate as shown in Fig. 1.[1] At the beginning of research and development work on metal/ceramic joining the chemical view predominated. However, considerable success in establishing reliable joining techniques was only then achieved when the mechanical behaviour of the bonded dissimilar materials and the influence of their thermomechanical properties including their moduli of elasticity, Poisson numbers, and thermal expansion coefficients were considered within the framework of fracture mechanics. Microstructural studies are necessary to include the effects of interlayer thickness, grain size, and flaws on the properties of the bonded system. Today, the atomistic structure of the metal/ceramic interface and its crystallographic orientation is experimentally investigated by high resolution electron microscopy. By simulation of the obtained electron image contrast informations can be gathered on the position, charge, and species of interfacial atoms.

Bond formation at the interfaces of metal/ceramic joints is despite the numerous experimental studies still not understood. Interfacial chemical reactions[2] contribute the main part to the adherence of metal/ceramic interfaces. The quality of a metal/ceramic bond depends also on the structure of the interface which is influenced by the mutual crystallographic orientation of the mating metal and ceramic surfaces.[3] The surfaces to be bonded should be free of adsorbed layers and oxides and in a defined condition in respect of their impurity content. To fulfill these demands new experimental approaches as for example ultra high vacuum bonding of sputter-cleaned surfaces of single crystals and polycrystalline materials must be utilized in fundamental research work. The formation of continuous and flaw-free interfaces and of thin interfacial reaction layers plays an important role for the technical applicability of metal/ceramic joints. Bonding temperature and time in active metal brazing and, additionally, bonding pressure in diffusion bonding, must therefore be optimised taking into account the different mechanisms which govern the elimination of interfacial voids and flaws.[4] With the knowledge gained from increased understanding of fundamental joining mechanisms new techniques are being developed and familiar ones are improved.[5] Further gains in an understanding of trends in metal/ceramic interface structure and bonding with alloy composition and segregation is expected from theoretical work using cluster and *ab initio* calculations[4] based on detailed and careful experimental studies.

This review paper on metal/ceramic joining is subdivided into sections on Active Metal Brazing and

Diffusion Bonding. Most of the information gathered in this article is taken from papers published in the last decade. Since many comprehensive review articles and surveys are available on brazing and diffusion bonding of metal/ceramic joints[2,6-9] and on metal/ceramic interfaces[10-14] the reader is recommended to refer to them for particular topics.

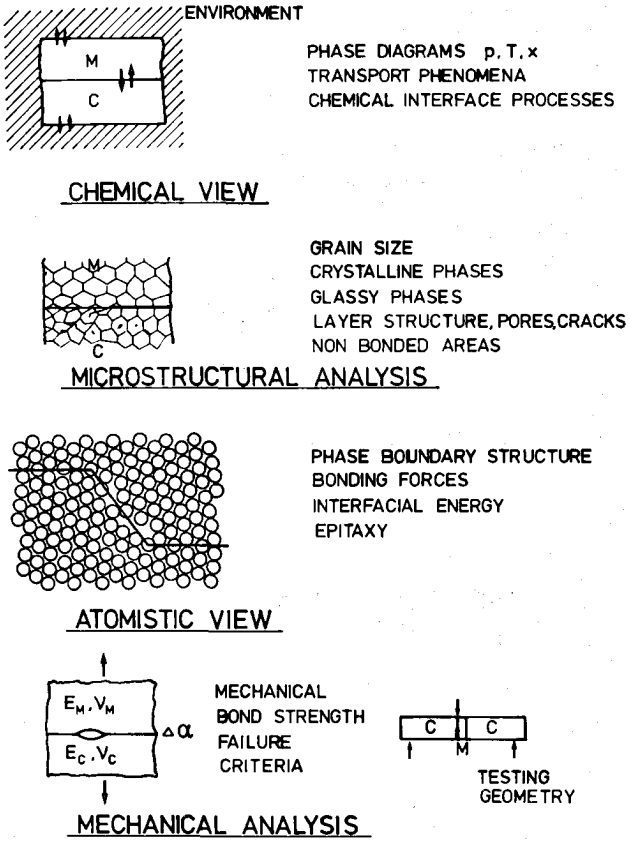

Fig. 1. Investigation methods for metal/ceramic joints.[1]

2. Active Metal Brazing

Intimate contact between the workpieces to be bonded is a prerequisite of successful joining. The conversion of the contacting surfaces into an atomically bonded interface is the next step to be achieved. Finally, this interface and its adjacent regions must be able to accomodate stresses due to thermal expansion mismatch between the metal and the ceramic. These stresses will be generated during cooling after bonding or under service conditions by temperature changes.

Molten brazes can be introduced between the mating surfaces of metals and ceramics to fulfill the condition of intimate contact providing they will wet them and penetrate into the irregularities of the surfaces. The poor wettability of ceramics is due to the ionicity and covalency of their lattices by which electron movement is restricted. If the braze alloy contains an element capable of changing the chemistry of the ceramic surface as with active brazes its ability to spread onto the ceramic, to wet, and to bond will drastically be improved. According to a schematic given by J. A. Pask[15] the active brazing process to join unmetallized ceramics to metals is compared in Fig. 2 to two classical processes in which the ceramic is first metallized and than bonded to the metal by a high temperature braze. The main technological advantage of active metal brazing is the fact that it is a one-step process. The TiH_2[16] process to metallize a ceramic consists of painting a slurry of the hydride onto the ceramic, drying and firing at a reduced pressure. The hydride decomposes and the Ti forms a coating on the ceramic. The second process to metallize a ceramic schematically illustrated in Fig. 2 is the well-known MoMn process in which a paint of Mo and Mn powder or of their oxide powders is applied to an Al_2O_3 or BeO ceramic and fired in H_2 of a controlled dew point. The Mo sinters to form a porous metal coating and the MnO reacts with the SiO_2 containing ceramic to form a glassy phase of controlled viscosity[17] which penetrates into the Mo coating. This coating is electroplated with Ni on

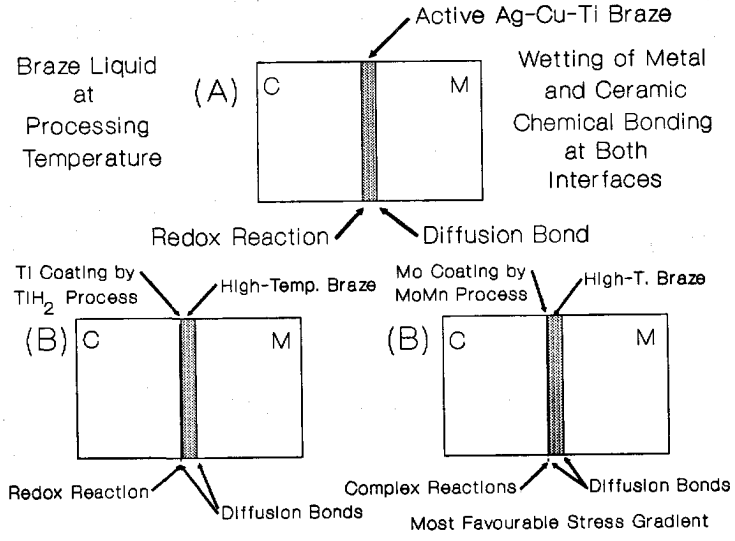

(A) Active metal braze in contact with unmetallized ceramic
(B) Braze in contact with metallized ceramic

Fig. 2.
Schematic after J. A. Pask[15] illustrating several conditions under which brazes are used.

which the braze spreads easily.

The most commonly used active metal additive is Ti.[18] Other active elements are V, Nb, Ta, Zr, Hf, and La which were already recommended more than 20 years ago in the patent literature.[19–21] Generally, Ag–Cu brazes contain only a small percentage of the active metal. An exception is pure aluminium which is used as an active metal braze for SiC and other ceramics.[22] Two basic mechanisms are involved in bond formation, solute metal segregation at the interface, and interface reaction. Bonding is mostly carried out in a high vacuum or in a neutral gas such as argon. The brazed components normally show reaction layers of some micrometers thickness at the braze/ceramic interface. If these reaction layers increase in thickness the bond strength of the joints can be degraded due to the formation of flaws in their microstructure and/or thermal expansion and volume mismatch promoting premature failure by interfacial stresses. Brazed joints do not withstand prolonged loading at high temperatures because reaction of the active metal with the ceramic will proceed.

Good braze alloys possess high thermodynamic activities for reactive elements as Ti. However, simply increasing the Ti concentration in the alloy is not useful. It leads to an increase in the liquidus temperature and thereby to an enhanced alloy embrittlement by reaction of Ti with oxygen from the atmosphere. The activity coefficient of Ti in a given alloy reacting with oxide ceramics can be substantially increased by adding alloying elements, such as In and Sn, that have low solubility for Ti.[23] Considerable attention has been paid to the Ag–27.5wt%Cu–2wt%Ti and Ag–24wt%Cu–15wt%In–1.5wt%Ti alloys[24] which melt at 780–795°C and 605–755°C and can be used at 820–860°C and 750–800°C, respectively. The quaternary alloy is described as a ductile braze.

2.1. *Oxide Ceramics*

Active element concentrations were optimized to obtain maximum bond strength values as shown for interfaces formed between alumina and several Ti containing alloys (Fig. 3[25]). The initial increase in bond strength with increasing active metal concentration is thought to be accompanied by the growth of islands of reaction products. At the optimum concentration a continuous thin interlayer of the reaction product is assumed to be formed.[25] An alternative explanation is a concentration dependent segregation of excess Ti atoms at the interface which are bonded to alumina without forming a bulk reaction product. Reduction of bond strength at higher Ti concentrations is explained by the formation of reaction layers of increasing thickness which weaken the joint due to their decreasing ability to accomodate volume mismatch and thermal contraction strains. The concentration of Ti in Cu based active brazing alloys is reduced by the addition of ternary alloying elements such as In[23] which decrease the Ti solubility but increase its activity and lead to an improvement of wettability.

Some studies contain informations on the nature of reaction products found at the oxide ceramic/metal interface. TiO was formed at 1 150°C by reaction between alumina and Cu–2at%Ti whereas Ti_2O_3 was formed at the same temperature by reaction between alumina and Au–2at%Ti.[26] Ti_2O_3 was also identified at the alumina/Ni–2at%Ti interface after brazing at 1 500°C.[26,27]

The work of adhesion W_{ad} in J/m² is a measure of the chemical bond strength at the metal/ceramic interface and can be expressed by the equation

$$W_{ad} = \gamma_M + \gamma_C - \gamma_{MC} \quad \text{.....(1)}$$

or for liquid metals in contact to solid ceramics according to the equation of Young $\gamma_C = \gamma_{MC} + \gamma_M \cdot \cos\theta$ by the equation

$$W_{ad} = \gamma_M(1 + \cos\theta) \quad \text{.....(2)}$$

where, γ_M, γ_C: the surface energy of the metal and the ceramic, respectively
γ_{MC}: the interfacial energy
θ: the angle of contact.

Naidich showed that there is a progressive improvement with increasing Ti/O ratio in the wetting behaviour for titanium oxide–copper interactions at 1 150°C reaching its minimum in contact angle for

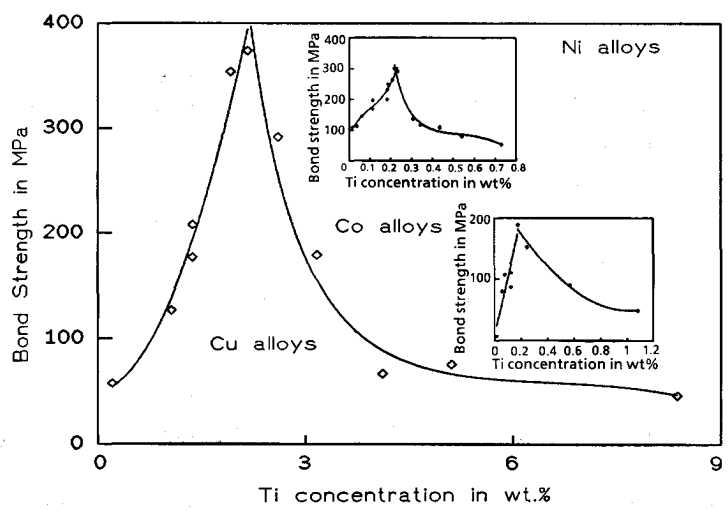

Fig. 3.
Tensile bond strength of joints formed between Ti-containing binary Cu, Ni, and Co alloys.[25]

titanium monoxide which is metallically bonded.[28] It was also experimentally demonstrated that the work of adhesion W_{ad} will be larger by a factor of about 2 if TiO is formed instead of Ti_2O_3 at the interface between oxides as Al_2O_3 and SiO_2 and active brazes based on Cu and Ni containing 2 at% Ti.[26] These observations can be explained by the fact that TiO possess metallic conductivity and metallic interatomic bonds wheras Ti_2O_3 is characterized by a considerable portion of ionic bonds as most of the structural oxide ceramics.

The McDonald and Eberhart model[29] which relies on calculations of atom–atom interactions suggests that a correlation exists between the work of adhesion W_{ad} and the bond strength measured in mechanical tests. This correlation was found for joints between pure metals and alumina fabricated by liquid metal bonding if W_{ad} values of solid/solid interfaces were used but was not confirmed for W_{ad} values of liquid/solid interfaces (Fig. 4[30]). Moreover, studies on joints between alumina and various binary Ni alloys manufactured by liquid metal bonding showed that a good correlation holds between the oxygen affinity of the solute metal and the tensile bond strength of the joints (Fig. 5[31]).

By raising the oxygen activity of the gaseous environment the contact angles of liquid metals on oxide ceramics can be lowered as shown by Chaklader *et al.*[32,33] for Cu, Ni, and Ag on alumina. These effects are attributed to the formation of the oxides $CuAlO_2$, $NiAl_2O_4$, and $AgAlO_2$ at the metal/alumina interfaces. Similarly, the direct bonding of Cu and alumina by formation of $Cu–Cu_2O$ eutectic is based on the presence of a certain oxygen activity.[34]

The bond strength of Al_2O_3/braze/Al_2O_3 joints was determined in three-point bend tests using 2.3 mm·2.5 mm·25 mm specimens. The composition of the braze alloy was Cu–44at%Ag–4at%Sn–4at%Ti. Brazing was performed at 800, 850, and 900°C in a high vacuum. Brazing time was varied between 5 and 20 min. The values of the mean bond strength of the brazed 99.5 wt% alumina ceramic specimens ranged between 80 and 120 MPa and showed only a slight dependence on brazing temperature and time.[35]

Bond strength values of 185 and 162 MPa were obtained for brazed Fe–29wt%Ni–18wt%Co/Al_2O_3

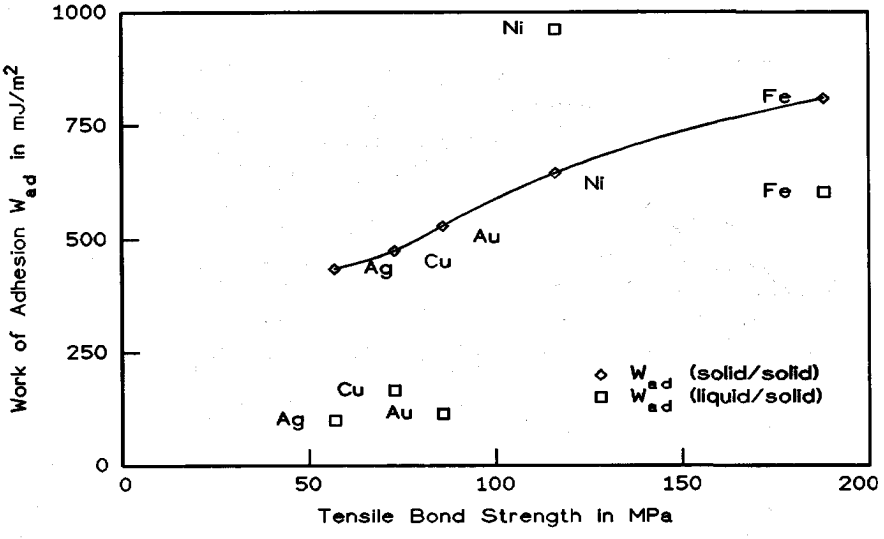

Fig. 4.
The room temperature tensile strength of metal/alumina joints and the work of adhesion W_{ad} for solid/solid and liquid/solid interfaces.[30]

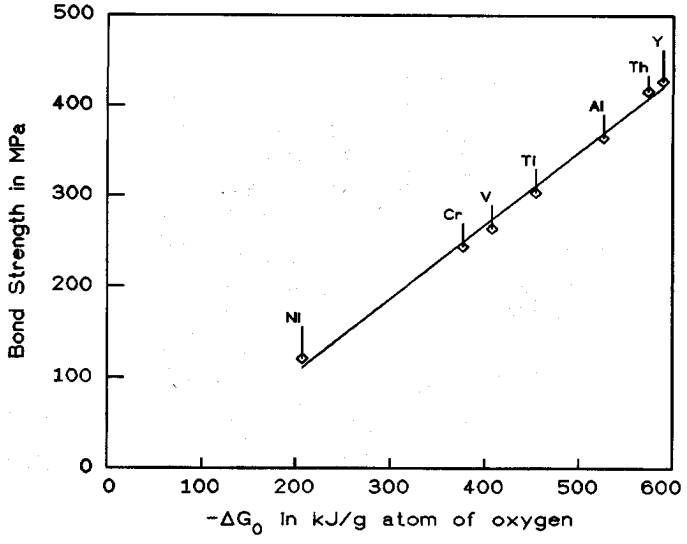

Fig. 5.
Tensile bond strength of joints formed between alumina and various binary Ni alloys as a function of the oxygen affinity $-\Delta G_0$ of the solute.[31]

joints with Ag–27wt%Cu–3wt%Ti and Ag–25wt%-Cu–15wt%In–1wt%Ti filler metals.[36] The thermal expansion behaviour of the Fe–Co–Ni alloy is nearly the same as that of the ceramic. The specimens 6 mm in diameter and 50 mm in length were examined in four-point bend testing. Fracture of the joints occurred mainly adjacent to the metal/ceramic interface within the ceramic.

Bond strength values of PSZ ZrO_2 joints brazed with a Cu–44at%Ag–4at%Sn–4at%Ti alloy at 800 and 850°C were larger than 400 MPa.[35] But the mean strength of PSZ ZrO_2 joints was only 248 MPa for specimens brazed at 900°C. At the PSZ interface a TiO interlayer was formed. To explain the large reduction in bond strength for specimens bonded at 900°C it was assumed that significant strains introducing damaging flaws were generated in the TiO layer. They are thought to be caused by an increase in the oxygen content at the PSZ interface and a corresponding difference in the lattice constant of the cubic TiO_x across the layer thickness.

Commercially available Ag–Cu–Ti and Ag–Ti brazes were used to manufacture metal/zirconia joints. The bond strength of the joints was determined in a shear test. The metal thickness was 10 mm and the thickness of the ceramic 4 mm. The brazed area was 20 mm·20 mm.[37] The materials used in this study were PSZ zirconia, TZP zirconia, and low carbon steel. Generally, the shear strength of brazed TZP ZrO_2/steel and PSZ ZrO_2/steel joints was larger than 100 MPa. However, TZP ZrO_2/steel joints fabricated by means of the most ductile Ag–4wt%Ti braze alloy at 1 050°C showed the lowest scatter in the measured bond strength values of 151±11 MPa which indicates the efficiency of thermal stress relief by plastic deformation. Brazing under argon or vacuum is recommended to achieve optimum wetting of the ceramic and avoid embrittlement of the braze alloy due to the affinity of Ti to oxygen and nitrogen in the atmosphere. The shear strength of the joints decreased with increasing ratio of ceramic thickness to metal thickness due to an increase of residual thermal stresses. The mean shear strength of TZP ZrO_2/Ag–Cu–1.5wt%Ti/steel joints was reduced from 144 to 109 MPa by increasing this thickness ratio from 0.4 to 1.0.

Microstructural examinations of active metal brazed zirconia joints revealed porosity within the braze besides migration of Ti to the bond interfaces and crack formation by thermal expansion mismatch. The bond strength values of zirconia/Ag–Cu–In–1.25wt%Ti braze/zirconia joints manufactured in a vacuum of 10^{-5} Torr at 770°C using partially stabilized zirconia (PSZ) specimens ranged between 131 and 372 MPa.[38] Bond strength was evaluated by four-point bend testing of 3 mm·3 mm·32 mm specimens with the braze centred in the middle. Shear testing has been used as a screening method to evaluate the bond strength of PLS ZrO_2/Ag–Cu–In–Ti braze/metal joints (PLS=pressureless sintered). The maximum shear strengths of 195, 170, 112, and 64 MPa were a function of the thermal expansion mismatch between the ceramic and the different metals Ti6A14V alloy, 446 stainless steel, gray cast iron and 21–2N stainless steel. Failure occurred at the ceramic/braze interface.

Moorhead and Becher[39] determined as a measure of bond strength fracture toughness values K_{Ic} of brazed zirconia joints in modified applied moment double cantilever beam (DCB) tests at room temperature. The metal composition of the brazing alloy was Cu–46at%Ag–4at%Sn–lat%Ti. Brazing was performed at 800°C under a vacuum of less than $7 \cdot 10^{-5}$ mbar. They obtained for PSZ ZrO_2/braze/PSZ ZrO_2 and PSZ ZrO_2/braze/Ti joints fracture toughness values of 7.4 and 9.9 MPa·$m^{1/2}$. The fracture toughness of the corresponding partially stabilized ZrO_2 ceramic was 14.0 MPa·$m^{1/2}$.

Studies on the bond strength at elevated temperatures were performed with Al_2O_3/Al/Al_2O_3 joints. The nominal tensile bond strength values of those joints with 40 μm Al interlayers after brazing at 1 000°C were 73 to 89 MPa at room temperature. The interfaces remained strongly bonded at 300°C and showed strength values of 89 to 117 MPa. Above 400°C the strength decreased appreciably with testing temperature.[40] Similar studies were performed with magnesia samples brazed with Al. The bond strength at room temperature was 40 MPa. Increasing the testing temperature leads to a decrease in strength to about 30 MPa at 500°C.[40] The slight increase in strength with increasing temperature and the decrease in strength above 400°C observed with Al_2O_3/Al samples were explained by the relaxation of residual thermal stresses within the ceramic and the ability of the metal layer to deform. The MgO/Al samples showed a slight decrease in bond strength with testing temperature presumably due to the formation of a brittle $MgAl_2O_4$ reaction layer and the porosity of the magnesia ceramic. Failure always occurred within the MgO ceramic.

2.2. *Joining Nonoxide Ceramics*

Silicon nitride or silicon carbide heat engine parts must be connected at some point to metal, for example, a ceramic turbocharger rotor to a metal shaft.[41] Methods have to be developed for hermetic packaging of electronic devices on AlN substrates by metal/AlN sealing. Nonoxide ceramics tend to be more highly reduced chemically than oxide ceramics, which effects interfacial reactions. Because most nonoxide ceramics have much lower thermal expansion coefficients than metals, braze techniques that use a ductile metal filler are preferred.

2.3. *Nitride Ceramics*

Active Cu–Ti alloy brazing of nitride ceramics to metals leads to the formation of TiN and intermetallic compounds between the metal element of the nitride and Ti at the interface. Formation of stoichiometric TiN should be avoided, since it is not wetted as a ceramic material by Cu. Experiments of Nicholas *et al.*[42] suggest that wetting and bonding of a Si_3N_4 ceramic by a Cu–Ti alloy with a minimum Ti

content of about 5 wt% is facilitated by the formation of Ti silicides which are of metallic nature.

Excellent wetting of AlN, BN, silicon nitride, and sialon ceramics by Ag–27wt%Cu–2wt%Ti was achieved at 950°C.[43] The bond strength of shear-tested Ag–Cu–Ti brazed Si_3N_4/Si_3N_4 joints was 270 MPa within the concentration range of 0.5 to 5 wt% Ti.[44] Reaction products identified by X-ray analysis at the interface of Si_3N_4/2.2wt%Ti–Ag–Cu were TiN, Ti_5Si_3, and $TiSi_2$. High resolution electron microscopy studies lead to the conclusion that fine TiN particles of 10 to 50 nm diameter are epitaxially grown along the wavy silicon nitride interface followed by a front of silicide particles. The TiN particles had a smaller lattice spacing than that of silicon nitride and might have helped in reducing internal stresses during cooling from the brazing temperature.

The four-point bend strength values of hot-pressed silicon nitride bonded to Fe–29wt%Ni–18wt%Co by Ag–28wt%Cu–2wt%Ti and Ag–25wt%Cu–15wt%In–1wt%Ti braze alloys were 95 and 51 MPa. Because of the large thermal expansion mismatch between the ceramic and the metal alloy these joints showed only half the bond strength measured by the same authors for brazed alumina/Fe–29wt%Ni–18wt%Co/Al_2O_3 joints.[36]

Bond strength values of Si_3N_4/Ag–Cu–In–1.25wt% Ti braze/Si_3N_4 joints manufactured in a vacuum of 10^{-5} Torr at 770°C using hot-pressed silicon nitride ranged between 219 and 427 MPa. Bond strength was evaluated by four-point bend testing of 3 mm·3 mm·32 mm specimens with the braze centred in the middle.[38]

Joining of silicon nitride ceramics was also studied using Ni–Cu braze alloys containing the active metal elements Cr, Nb, V, and Al.[45] High shear strength values of more than 280 MPa were obtained for pressureless sintered silicon nitride brazed with an Cu–10wt%Ni–1wt%V–1wt%Al alloy in a vacuum at 1 150°C/15 min. The thickness of interlayer foils made from this alloy was 140 μm. The dimensions of the bonded area were about 12 mm·12 mm and the height of the Si_3N_4 pieces 12 mm. Fracture occurred within the bulk of the ceramic. An increase in strength from 169 to 247 and 251 MPa, respectively, was observed for brazed Si_3N_4/Cu–10wt%Ni–1wt%V/Si_3N_4 joints when Al or Ti had been deposited onto silicon nitride prior to bonding. Argon atmosphere lead to a considerable decrease in bond strength with the exception of joints brazed with the Al–V–Ni–Cu alloy. X-ray diffraction analysis showed that nitrides and silicides of the metals Cr, Nb, or V were formed in the reaction layer.

Aluminium is also an active braze to bond nitride ceramics to metals. The interfacial layers obtained after Al-brazing consist of SiAlON phases and AlN.[46] Nitride ceramics AlN, BN, Si_3N_4, and sialon showed a good wettability by Al melts at temperatures above 1 000°C. The most easily wetted ceramics were the sialons.[43] TEM studies revealed the presence of a thin β' sialon layer at the silicon nitride side of the Al/Si_3N_4 interface region.[46] It consisted of fine particles which were about 8 nm in diameter. The bond strength values of Al/nitride ceramic joints measured in shear tests ranged from 6 MPa for BN to 61 MPa for a sialon ceramic.[43] The fracture resistance K_C of Si_3N_4/Al joints bonded at 860°C was 5.5 MPa·$m^{1/2}$ which was almost identical with the fracture resistance of the monolithic ceramic. The bond strength was 370 MPa.[47] This value was obtained in four-point bend tests at a cross-head speed of 0.5 mm/min using specimens of the dimensions 3 mm·3 mm·38 mm. A strong strain-rate dependence of the bond strength was observed.

Steel/Invar/Al/Si_3N_4/Al/Invar/steel joints were brazed at 800°C/0.15 MPa/7 min in an argon flow using diffusion bonded Invar/steel pieces.[48] The Si_3N_4 disc was 1 mm in height and 7 mm in diameter. The Invar/steel parts of same diameter were produced from Invar disks 2 mm in height and steel pieces 5 mm in height. The initial thickness of 0.5 mm of the Al interlayers was reduced to about 0.05 mm after brazing. The brazed specimen had a tensile strength of more than 70 MPa. This value is equal to the strength of the adhesive used for bonding the tensile shoulders. Bend test specimens of dimensions 2 mm·2 mm·15 mm were cut from the joints. Their strength values measured by four-point bending were 160 to 200 MPa. The specimens fractured along the steel/Al interface at which a brittle intermetallic compound had been formed during brazing. Steel/Al/Si_3N_4 joints were also brazed at 800°C/0.15 MPa/7 min. They showed only tensile strength values between 7 and 10 MPa and fractured at the Si_3N_4/Al interface. A comparison of the strength data indicates that a high bond strength between Si_3N_4 and Al will be achieved if the thermal expansion mismatch between steel and the ceramic is reduced by the introduction of an interlayer possessing nearly the same thermal expansion behaviour than the ceramic. Invar fullfils this condition.

Prior to the brazing operation pressureless sintered silicon nitride was metallized with Al at 1 100°C/1 h and Fe, Cu, and stainless steel were electroplated with a Ni layer of 60 μm thickness.[49] Lap joints of the ceramic bonded to the Ni-plated metals and to Nb, Ti, and Cu were manufactured by brazing at 800°C using an Al filler metal foil of 100 μm thickness. The diameter of the silicon nitride pieces was 15 mm and their thickness 3 mm. The metal disks were 6 mm in diameter and 3 mm in thickness. The strength of Si_3N_4/Al/metal joints determined by shear fracture loading decreases with increasing $\alpha \cdot E$ due to imposed thermal residual stresses. α is the thermal expansion coefficient and E the modulus of elasticity of the metals. Si_3N_4/Al/Nb and Si_3N_4/Al/Ti joints showed the highest bond strength values of about 100 MPa. Wetting was achieved by the formation of AlN type sialon at the interface of silicon nitride. Within the Al filler metal $NbAl_3$ or $TiAl_3$, respectively, is formed by reaction with Nb or Ti.

Results of stress distribution obtained by finite element calculations based on elastic deformation of joints were compared with residual stress measure-

ments on Al-brazed Si_3N_4/Invar (or Kovar) joints by means of a strain gauge method.[50] In the rectangular joints with a bonded interface of 15 mm·20 mm the highest tensile stresses were found at the edge of the ceramic near the interface in agreement with FEM calculations. In cylindrically shaped joints these stresses increased with increasing bonding area. The residual thermal stresses introduced flaws into the ceramic near to the interface by which the joints were weakened. Because of the larger thermal expansion coefficient of Kovar the bond strength of Si_3N_4/Kovar joints was considerably lower and the Weibull modulus was larger than the corresponding values of Si_3N_4/Invar joints.[51] Both types of joints were brazed at 800°C/0.15 MPa/7 min under flowing argon. The weak Kovar joints fractured partially at the Si_3N_4/Al braze interface whereas the strong Invar joints which showed a strength of about 150 MPa failed in the reaction layer at the Al/Invar interface.

Si_3N_4/Al/Si_3N_4 joints were produced by Al brazing at 800°C/0.05 MPa/10 min in flowing Ar gas. The Al filler was 99.9 wt% pure and 0.5 mm thick.[52] After bonding the thickness of the Al layer was between 10 and 20 μm. The silicon nitride used contained 10 wt% Al_2O_3, MgO, and Y_2O_3 additives and was in the form of disks 13 mm in diameter and 7 mm high. To study the effects of surface damage on the strength of the joints ceramic surfaces of three grades of roughness were prepared. Their average values R_a were 0.1, 0.2, and 0.3 μm. Bend test specimens of 1.7 mm high by 2.5 mm wide by 15 mm long were cut from the bonded pieces. The statistical treatment of the results obtained by three-point bend tests revealed an decrease in average bond strength and Weibull parameter m with increasing R_a. The corresponding strength values were 470, 355, and 270 MPa and the m values were 20, 12, and 3, respectively. The average bend strength and the m value of the as received silicon nitride were 554 MPa and 20. Joints produced from smooth surfaces fractured within the Al filler. The obtained results demonstrated that damage introduced into the surface of the ceramic by grinding operations reduced the strength and lead to a considerable scatter in the bond strength data. However, specimens made from polished ceramic surfaces containing less flaws showed high strength values of less scatter.

2.4. *Carbide Ceramics*

The active metal brazing has also been studied fairly extensively for joining carbide ceramics. Pieces of sintered SiC of the dimensions 10 mm·24 mm·50 mm were joined using Ag–27wt%Cu–3wt%Ti foils of 200 μm thickness as interlayers. SiC/Ag–Cu–Ti/SiC and SiC/Ag–Cu–Ti/Cu/Ag–Cu–Ti/SiC configurations of the bonded joints were manufactured.[53] Bonding was achieved both by brazing and by diffusion welding at 950°C/5 min and at 850°C/5 min/15 kPa, respectively, in a vacuum of $5 \cdot 10^{-7}$ mbar. EPMA studies suggested that silicides and carbides are formed at the SiC interfaces. The brazed and the diffusion welded joints showed only low bond strength values of about 100 MPa. They were measured in four-point bend tests.

Pressureless sintered (PLS) SiC containing about 1 wt% free C and B showed a good wettability for Ag–Cu–Ti brazing alloys.[54] The bond strength of SiC/braze/SiC sandwich configurations increases with decreasing Ti content of the braze. The shear strength values of joints manufactured at 950°C/5 min were 15 MPa for an 8 wt% Ti alloy and 70 MPa for a 2 wt% Ti alloy. The latter SiC/braze/SiC joints were also cut into bars of 3 mm·3·5 mm·36 mm and tested in four-point bending. Their bond strength was about 370 MPa. Additionally, thermal shock tests showed that quenching from 400°C did not reduce the bond strength.[55] High-resolution electron microscopy studies showed that a TiC reaction layer was formed at the interface of SiC/SiC joints brazed by an Ag–28wt%Cu–2wt%Ti alloy specimens at 950 °C/30 min. Their high bond strength values were attributed to the formation of an epitaxial interface between SiC and TiC with crystallographic relations of (0006)SiC || (111)TiC and $[10\bar{1}0]$SiC || $[1\bar{2}1]$TiC. The corresponding d-spacings of SiC and TiC differed by not more than 3 %.[56] Reaction products between an Ag–Cu–2%Ti brazing alloy and sintered SiC are TiC, Ti_5Si_3, and Ti_3SiC_2.[54] The wettability of the reaction products is nearly the same as that of SiC which suggests that Ti in the brazing alloy mainly promotes wetting by interfacial adsorption processes which lower the interfacial energy. For the reaction products and for SiC values of thermal expansion coefficients, Vickers microhardness at 500 gf load and four-point bend strength for 3 mm·4 mm·25 mm specimens at a cross-head speed of 0.5 mm/min were determined and are given in Table 1. The formation of mechanically weak reaction products such as Ti_5Si_3 leads to a reduction of bond strength. Because of the high values of thermal expansion coefficients of the reaction products, which were twice that of SiC, thermal stress is generated between SiC and the reaction layer, which will increase with increasing thickness of the reaction layer and lowers the bond strength. Therefore, the reaction layer must be kept as thin as possible.[54] It was observed that Ti_3SiC_2 interlayers in SiC/Ti/SiC joints were plastically deformable.[57] These joints were diffusion bonded at 1 450°C/1 h/30 MPa after sputtering Ti layers of 0.2 to 3 μm thickness onto SiC. Their bond strength was 286 MPa measured in four-point bend tests.

PLS SiC was applied in joining SiC/Al/SiC

Table 1. Properties of SiC and SiC/Ag–Cu–2wt%Ti reaction products.[54]

Material	Theor. density (%)	Thermal expansion coefficient (K^{-1})	Vickers hardness	Bend strength (MPa)
SiC	98	$4.7 \cdot 10^{-6}$	3 000	430
TiC	96	$8.2 \cdot 10^{-6}$	3 000	510
Ti_5Si_3	99	$9.5 \cdot 10^{-6}$	970	70
Ti_3SiC_2	95	$9.2 \cdot 10^{-6}$	750	400

specimens at 1 000°C in vacuum for a few minutes by induction heating. The thickness of the active Al interlayers was 0.5 mm prior to bonding. The bond stregth of these joints measured at room temperature in four-point bend tests was about 240 MPa.[22] TEM and HREM (high resolution TEM) studies showed that aluminium carbide Al_4C_3 was formed at the metal/ceramic interface and that an epitaxial relation between this interlayer and Al of (111)Al || (0001)-Al_4C_3 and $[1\bar{1}0]Al || [10\bar{1}0]Al_4C_3$ was observed. A disadvantage of the presence of aluminium carbide is its tendency to be corroded by water.[58] A bend test specimen with an Al_4C_3 reaction interlayer was completely broken after it was immersed for 100 h in water at room temperature. Aluminium carbide was not detected at the interface of joints between Al and reaction-bonded SiC containing free Si.[22] However, their bond strength values were only 110 PMa at room temperature.

Hot-pressed SiC was bonded to steel by an Ag–4wt%Ti braze alloy and an Mo interlayer of 2 mm thickness which served to reduce residual stresses due to thermal expansion mismatch between the ceramic and steel.[59] The brazing temperature was 1 050°C. The bond strength was measured in four-point bend tests using specimens of dimensions 4.5 mm·3.5 mm·42 mm. The obtained bond strength values ranged between 120 and 150 MPa. SiC/Ag–4wt%Ti braze/steel joints showed only bond strength values of 50 to 70 MPa. The strength of the monolithic SiC was 535 MPa. This study also demonstrated that Ag–Cu–Ti brazes were not suitable to join SiC to Mo because these alloys react strongly with Mo.

PLS SiC plates of 10 mm·10 mm·4 mm were joined to stainless steel rods of 5 mm thickness and 5 mm height by means of an Ag–28wt%Cu–1.5wt%Ti braze alloy inserted as a powder mixture.[60] A maximum shear strength of 135 MPa was measured after brazing at 825°C for a holding time of 0 min. The rates of heating and cooling were 50 and 60 K/min, respectively. Fracture occurred within the ceramic. The strength increased with decreasing brazing temperature and holding time in the intervals 825 to 950°C and 0 to 60 min. However, joining was unsuccessful when the steel rod was replaced by a larger steel plate of dimensions 10 mm·10 mm·4 mm. The specimens failed by the formation of cracks in the SiC ceramic due to the large thermally induced stresses during cooling of the joints. Optimum release of residual stresses was achieved by the insertion of a double layer of Ti and Mo each of 0.5 mm thickness between SiC and stainless steel and brazing with Ag–28wt%Cu alloy foils at 810°C. The SiC/Ti/Mo/stainless steel joints showed a maximum shear strength of 50 MPa which can be attributed to a reduction of thermal expansion mismatch by the layer configuration ceramic/interlayer 1/interlayer 2/metal which obbeys the condition $(\alpha_C = \alpha_1 > \alpha_2) < \alpha_M$. A thin layer of Ti_3SiC_2 was observed at the SiC/braze interface of joints brazed for very short times. However, with increasing bonding temperature and time Ti_5Si_3 containing carbon and TiC_x were formed by reaction of SiC with Ti supplied from the braze side which are assumed to lower the bond strength.

3. Diffusion Bonding

Diffusion bonding is a solid-state joining process by which two nominally flat surfaces are joined at an elevated temperature under a low mechanical pressure in a high vacuum, in an inert atmosphere, or in an atmosphere of defined oxygen or nitrogen activity. The temperature is usually in the region of 0.5–0.95 $T_m \cdot T_M$ is the melting point or the temperature of the melting range of the metal part in K. The technological advantages of diffusion bonding are low deformation which enables parts to be joined without distortion, the ability to join large areas, the applicability of diffusion bonded joints at high service temperatures, and possibilities for joining materials in nonconventional situations. Diffusion can take place along or across the metal/ceramic interface. The materials to be bonded are generally rather complex in chemical composition and part of their impurities tend to be segregated at the surfaces and interface. When metal/ceramic joints are diffusion bonded, two major groups of bond will be observed. A well-defined interface is found for the noble metals Au, Ag, and Pt and for the reactive metal Nb bonded to alumina. In many other cases a reaction occurs between the ceramic and the metal, *e.g.*, between Zr and silicon nitride, producing a second phase at the interface. The second phase often weakens the interface. As with joints brazed by the active metal method the bond strength of diffusion bonded joints is strongly affected by thermomechanical mismatch between the metal and ceramic. The main information obtainable in current literature concerns with bond strength determination as a function of the bonding variables and with an analysis of the reaction products found at the metal/ceramic interfaces.

Diffusion bonding requires that the materials are brought into intimate contact so that their atoms are within interatomic distance. To fulfill this condition the surfaces of the metals and ceramics must be clean and free from impurity atoms and adhering films. Moreover, the surrounding atmosphere interacting with the free surfaces of the materials must be clearly defined. If chemical reactions are excluded the driving force for an interface formation would be the energy set free as soon intimate contact is achieved. This energy is the work of adhesion W_{ad} required to separate the solid/solid interface into the surfaces of the solid metal and ceramic. Chemical reactions will further lower the free energy of the system. Although a metal/ceramic joint is always in a state of chemical nonequilibrium thermochemical equilibrium considerations (2) are indispensable for the description of reactions occurring between both materials and their environment under standard and nonstandard conditions.

J. T. Klomp noticed that, *e.g.*, the reaction between Ni and Si_3N_4 given by the equation

$$1/3\ Si_3N_4 = [Si]_{Ni} + 2/3\ N_2$$
$$\Delta G^\circ = 51\,945 - 30 \cdot T \text{ in cal/g atom Si} \quad \text{.....(3)}$$

depends on both temperature and N_2 pressure of the environment. $[Si]_{Ni}$ denotes Si dissolved in Ni. Reaction will occur if the N_2 pressure is lowered beyond its equilibrium pressure thus enabling an uptake of Si into the Ni solid solution. At 1 000°C the N_2 pressure must be below 10 mbar and the Si content of Ni about 1 at% or less. Only if the nonmetallic element of the ceramic is oxygen or nitrogen the metal/ceramic reaction can be controlled by the surrounding gaseous atmosphere by means of the oxygen or nitrogen activity.

If possible, an excessive formation of layers composed of brittle interfacial phases should be avoided by the introduction of ductile metal interlayers or layers of diluted alloys where an active solute diffuses to the interface and reacts with the ceramic. In both cases the gradient of the thermodynamic potential is very small in comparison to that of the active metal as a bulk.

The kinetics of the metal/ceramic reaction and interface formation can only be determined experimentally. Mechanical pressure applied during diffusion bonding to produce plastic deformation of the metal will never produce full interfacial contact. Other mechanisms must operate to close residual interfacial pores. Collapse of pores can be achieved by vacancy diffusion in the metal along the interfaces. The shrinkage of pore volume V is given by the relation (2)

$$-dV/dt = 8 \cdot \pi \cdot D \cdot \gamma_M \cdot \Omega/(k \cdot T) \quad \text{.....(4)}$$

where, D: the coefficient of vacancy diffusion
γ_M: the surface energy of the metal
Ω: the vacancy volume.

Similar relations have been applied for Al/Al_2O_3 joints[61] in which the size of a circular pore and the effect of external pressure are included. A displacement of the interface occurs in reactive metal/ceramic systems. For ternary and higher order systems the boundary shape can change from planar to nonplanar interfaces.[62,63]

3.1. *Model Combination* Nb/Al_2O_3

The influence of the interfacial microstructure on the bond strength was studied using diffusion bonded Nb/Al_2O_3 joints.[64,65] This system was chosen as a model combination because of its negligible thermal expansion mismatch and its solid-solution reaction $Al_2O_3 = 2[Al]_{Nb} + 3[O]_{Nb}$ in a high vacuum at elevated temperatures by which a formation of interfacial reaction layers will be avoided. $[Al]_{Nb}$ and $[O]_{Nb}$ denote Al and oxygen dissolved in Nb. Polished polycrystalline Nb (99.8 wt%) sheets of 1 mm thickness, sapphire crystals of 99.9 wt% purity in the form of 1 mm thick disks, and polycrystalline alumina pieces (99.7 wt% Al_2O_3, 0.3 wt% MgO) of dimensions 14 mm·20 mm·15 mm were used in the bonding experiments. From the welded joints four-point bend test specimens were cut and notched at one ceramic/metal interface. Typical dimensions of the specimens were 2 mm·5 mm·34 mm. The fracture energy G_c[66] was taken as a measure of bond strength. $Al_2O_3/Nb/Al_2O_3$ joints prepared from alumina pieces with either diamond-cut, ground (diamond grain sizes 64 and 20 μm) or polished (diamond grain size 1 μm) surfaces were manufactured at 1 700°C/10 MPa/2 h in a high vacuum of 10^{-5} mbar.[64] The degree of bonding given by $P_H = (A_b/A_t)$, where A_b is the projected bonded area and A_t the total interface area, was measured at the interfacially fractured surfaces under the scanning electron microscope. Joints made from the polished ceramic pieces showed the highest fracture energy of 55 J/m² and a P_H value of 100 %. The fracture energy of joints produced from as-cut alumina pieces was only 25 J/m² and its degree of bonding 63 % indicating that surface roughness and defects introduced by surface machining of the ceramic will cause incomplete bonding and will reduce the bond strength of the joints. To get informations on the influence of metal grain growth during welding on the bond strength polished Nb sheets of initial grain sizes 390, 400, 480, and 630 μm were bonded to $(1\bar{1}00)$ planes of polished sapphire disks.[65] Bonding of the $Al_2O_3/Nb/(1\bar{1}00)$ sapphire/Nb/Al_2O_3 joints was performed at 1 700°C/10 MPa/2 h. The fracture energy G_c decreased with increasing initial Nb grain size but increased with increasing grain growth which is given by the difference between final and initial grain size. An optimum fracture energy of 55 J/m² was obtained after a grain growth of 377 μm from an initial grain size of 13 μm whereas joints manufactured from Nb sheets of 630 μm initial grain size showed only a Nb grain growth of 27 μm and a G_c value of 10 J/m². The beneficial effect of metal grain growth was assumed to be caused by an accomodation of the interface structure between each grain and the mating sapphire plane resulting in a low energy configuration of high fracture energy. First diffusion bonding experiments using single crystal Nb/sapphire couples performed by M. Turwitt *et al.*[65] showed that the fracture energy depended on the crystallographic character of the interfaces.

Single crystals of Nb of 99.9 wt% purity and of sapphire of 99.9 wt% Al_2O_3 purity were diffusion bonded at 1 700°C/10 MPa/2 h in a vacuum of $1.3 \cdot 10^{-6}$ mbar. The orientation relationship $(110)Nb \parallel (0001)Al_2O_3$, $[001]Nb \parallel [2\bar{1}\bar{1}0]Al_2O_3$ was adjusted with an experimental accuracy of ±1°. Two specimens of orientations I and II were cut and thinned from these joints with the foil normals parallel to $[001]Nb \parallel [2\bar{1}\bar{1}0]Al_2O_3$ and $[1\bar{1}0]Nb \parallel [01\bar{1}0]Al_2O_3$, respectively. Florjancic *et al.*[67] demonstrated that the near-interface regions can be imaged by high resolution electron microscopy. The lattice image revealed that the Nb/Al_2O_3 interface lay parallel to the close-packed plane of Al_2O_3. Lattice distortions occurred only in about 4 atomic layers of Nb adjacent to the interface. Moreover, the HREM images showed that no intermediate interlayer, *e.g.*, an oxide or spinel layer, was formed during diffusion bonding in accordance with the solid solution reaction between alumina and Nb

which will take part during diffusion bonding. It was argued if NbO_x interlayers of a thickness up to about 10 μm as described in a similar work of Morozumi *et al.*[68] or other types of reaction layers were to exist one should be able to resolve them by diffraction studies in the electron microscope. However, detailed diffraction studies were performed in which no diffraction spots of NbO_x or of other compounds could be observed.

High resolution electron microscopy (HREM) studies of the interface of an Al_2O_3/Nb joint were performed.[69] A single crystal of alumina of diameter 50.8 and 2 mm in thickness sliced parallel to $(01\bar{1}2)$ was bonded to a polycrystalline Nb sheet of 99.9 wt% purity at 1 600°C/12 MPa/1 h in a high vacuum. A 0.15 μm thick reaction layer was found at the Nb/Al_2O_3 interface. The chemical composition of this layer, its lattice constant and structure lead to the conclusion that hibonite, $CaO \cdot 6Al_2O_3$, had been formed at the interface. EDX analysis revealed that Ca was below the detection limits in both bulk alumina and bulk niobium. But ion microanalysis (SIMS) showed that Ca was the third major impurity after Al and Na at the surface of niobium. It was concluded from HREM investigations that the epitaxial relationship $(01\bar{1}2)Al_2O_3 \,||\, (0002)CaO \cdot 6Al_2O_3$ holds for the hibonite reaction layer whereas the $CaO \cdot 6Al_2O_3$/Nb interface appeared to be non-epitaxial. The formation of the hibonite layer was thought to be significant in relieving interfacial thermal stresses.

To study the annealing characteristics of flaws in diffusion bonding of Nb to alumina Nb surfaces were prepared so that arrangements of linear defects, about 10 μm wide and 1 μm deep were included.[70–72] Furthermore, interfacial pores were modelled by hardness indentations introduced into the Nb and sapphire surfaces to be bonded. Bonding of Al_2O_3/Nb/Al_2O_3 was performed under well defined conditions of temperature, time, vacuum, bonding pressure, and cooling rate. The displacement of the metal/ceramic interface deduced from the experimentally obtained concentration profile of Al in Nb was 0.9 μm after bonding at 1 850°C/10 MPa/2 h. The change of the structure of the flaws was analysed after decohesion of the partially bonded interface. It was shown that the closing of the flaws depended on the chemical reaction rate of the solute solution process of Al_2O_3 into Nb, the diffusion mechanisms in Nb, and the Al_2O_3 condensation at interface flaws. The applied bonding pressure of 10 MPa at bonding temperatures between 1 250 and 1 850°C lead to plastic deformation of the metal part by creep but did not cause measurable material transport at the metal/ceramic interface.

3.2. *UHV Bonding*

To prevent interface contamination during diffusion bonding of metal/ceramic joints an apparatus has been built which allows single crystals to be bonded in accurately predetermined mutual orientation and with controlled surface cleanliness in an ultra high vacuum.[3,73] Fig. 6 shows a schematic of the UHV facility for diffusion bonding. The surfaces of the crystals are cleaned by bombardment with 3 keV Ar ions. An Auger analyser monitors residual surface impurities. The cleaned crystals are transferred to a separate welding chamber in which they are succesively centred and stacked on an alumina plunger, azimuthally adjusted and preloaded. Bonding is initiated by raising the stack into the heating zone and applying the bonding load. The vacuum is typically $<2 \cdot 10^{-10}$ mbar. During heating the pressure climbs to around $2 \cdot 10^{-8}$ mbar. The maximum bonding temperature is 1 800°C. In the surface doping chamber on the right controlled contamination can be applied to the cleaned surfaces by electron-beam evaporation from a source prior to bonding thus enabling the study of the influence of impurities on the interface structure and bond strength.

Bonding experiments using single crystal couples and polycrystalline combinations of Nb/Al_2O_3 and Cu/Al_2O_3 were performed in the newly constructed

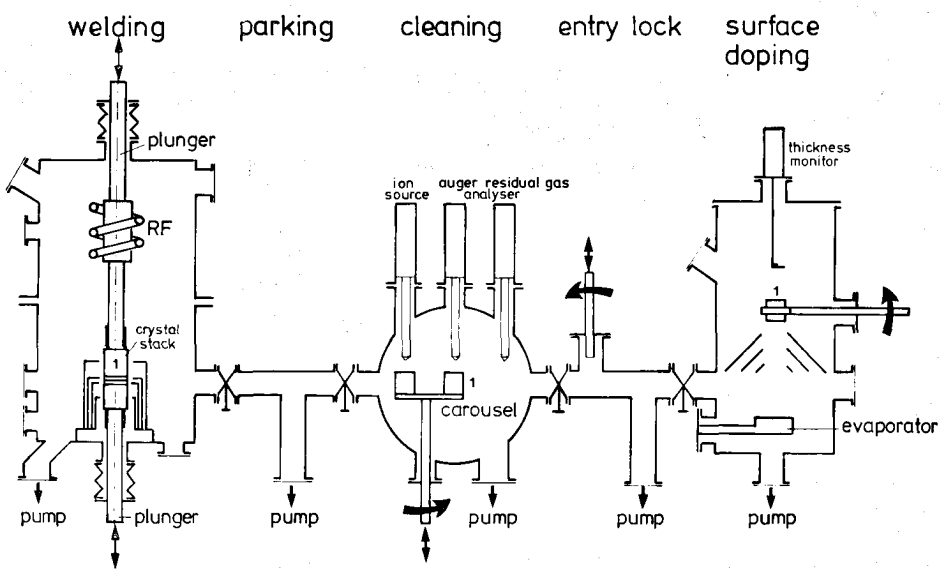

Fig. 6. UHV facility for diffusion bonding of oxide/metal bicrystals with controlled interface purity.[3]

ultra high vacuum facility.[74] Polycrystalline Nb/Al_2O_3 and Cu/Al_2O_3 joints were manufactured from polished Nb (99.99 wt%) and Cu (99.99 wt%) sheets of 2 mm thickness and 15·20 mm² surface area and from polished (1 μm diamond paste) alumina pieces of 99.7 wt% Al_2O_3 purity and of dimensions 15·15·10 mm³. Similarly, joints were made from crystallographically preoriented and polished Nb and sapphire single crystal disks of 1.5 to 1.8 mm thickness. The chemical composition of the Nb crystals was 99.999 wt% Nb, 150 ppm oxygen, and 50 ppm nitrogen. The sapphire crystals were of 99.99 wt% purity. The polycrystalline Al_2O_3/Nb/Al_2O_3 and Al_2O_3/Cu/Al_2O_3 joints were fabricated from sputter-cleaned metal and alumina pieces and UHV bonded for 1 h under a pressure of 16 MPa. The bonding temperatures were varied between 1 010 and 830°C (Cu/Al_2O_3) and 1 450 and 920°C (Nb/Al_2O_3). Triple interlayers of single crystals Nb/sapphire/Nb were bonded to two polycrystalline alumina endpieces of 15·10·15 mm³ at 1 300°C/6.5 MPa/1 h (Nb/Al_2O_3) and 900°C/6.5 MPa/1 h (Cu/Al_2O_3). From each welded piece a maximum of 6 bend test specimens of approximate dimensions 4 mm·2 mm·30 mm was obtained. The specimens were notched at one of their metal/ceramic interfaces. Four-point bend tests were performed at a cross-head speed of 0.1 mm/min. Fracture energy data were evaluated as a measure of bond strength according to a method developed by T. Suga and G. Elssner.[66] The interface fracture energy G_c decreased with decreasing bonding temperature for polycrystalline Nb/Al_2O_3 from 110 to 12 J/m² and for Cu/Al_2O_3 from 143 to 58 J/m². This effect was caused by a reduction of intimate contact between the mating surfaces during welding. Material transport at interface voids and local plastic deformation is impeded at lower bonding temperatures. For Nb/Al_2O_3 joints intimate contact between both materials is additionally assisted by the dissolution of Al_2O_3 into Nb which again is reduced by lowering the reaction temperature. Nevertheless, the G_c value of 72 J/m² obtained from Nb/Al_2O_3 joints UHV bonded at 1 310°C is appreciably larger than the G_c value of 43 J/m² obtained from a Nb/Al_2O_3 joint bonded in an ordinary high vacuum at 1 600°C. TEM observations showed that no reaction layers were formed at the UHV bonded Nb/Al_2O_3 and Cu/Al_2O_3 interfaces. The fracture resistance values K_c calculated from the obtained fracture energy values of the UHV bonded Cu/Al_2O_3 joints were somewhat larger than those obtained from Cu/Al_2O_3 joints bonded in a H_2/N_2 atmosphere,[75] *e.g.*, 4.7 MPa·m$^{1/2}$ after UHV bonding at 920°C and 4.3 MPa·m$^{1/2}$ after H_2/N_2 bonding at 950°C. Table 2 shows the results of fracture energy measurements on notched single crystal Nb/Al_2O_3 couples. They confirmed the strong orientation dependence of the interface fracture energy. Maximum G_c values were measured for interface orientation 1 (see Table 2) where the interface could not be fractured. Orientation 1 is the same as that of an interface formed *in situ* by internal oxidation between particles of α'-Al_2O_3 particles and the Nb matrix.[3] The AES spectra from bonded regions of polycrystalline Nb/Al_2O_3 joints showed a large oxygen peak due to the reaction between Nb and Al_2O_3. The thickness of a layer enriched in oxygen was about 5 nm. Nearly the same amounts of impurity atoms S, Cl, Ca, and C were found at bonded and unbonded regions.

Table 2. Values of fracture energy energy G_c of UHV bonded Na/Al_2O_3 joints manufactured from Nb and sapphire single crystals of different crystallographic orientation by UHV bonding at 1 300°C/1 h.[74]

No.	Orientation of interface planes and directions	G_c (J/m²)
1	(110) Nb || (0001) Al_2O_3, [001] Nb || [1$\bar{1}$00] Al_2O_3*	2 390*
2	(110) Nb || (11$\bar{2}$0) Al_2O_3, [001] Nb || [0001] Al_2O_3	2 330
3	(110) Nb || (0001) Al_2O_3, [001] Nb || [11$\bar{2}$0] Al_2O_3	182
4	(110) Nb || (1$\bar{1}$00) Al_2O_3, [001] Nb || [11$\bar{2}$0] Al_2O_3	175
5	(100) Nb || (11$\bar{2}$0) Al_2O_3, [001] Nb || [0001] Al_2O_3	101
6	(100) Nb || (1$\bar{1}$00) Al_2O_3, [011] Nb || [11$\bar{2}$0] Al_2O_3	100
7	(100) Nb || (0001) Al_2O_3, [001] Nb || [11$\bar{2}$0] Al_2O_3	68

* Specimens fractured at the unnotched polycrystalline Nb/Al_2O_3 interface.

Ultrahigh vacuum bonding experiments without any heating process were performed by T. Suga *et al.* to obtain joints between aluminium and sintered Al_2O_3, sapphire, Si_3N_4, or AlN.[76] This method is based on the idea that strong bond forces can develop at the metal/ceramic interface when 2 clean solid surfaces are brought into contact. Moreover, residual thermal stresses could be avoided because thermal expansion mismatch between the metal and the ceramic will not exist when both materials are bonded at room temperature. Flat polished ceramic plates of 3 mm height and 15 mm cross-section and Al discs of 5 mm height and 7 mm cross-section were used. The bonding surfaces of the metal were lapped and electrochemically polished to obtain a curvature of 25 mm. Prior to bonding the surfaces of the specimens to be joined were sputter-cleaned for 20 min by a neutral Ar beam at an energy of 1.5 keV. Immediately afterwards the specimens were brought into contact for 20 s using loads between 600 and 900 N. Bonding was performed in an ultra high vacuum of 10^{-10} mbar. The contact pressure of about 200 MPa deformed the metal plastically. The bonded area ranged between 3 and 7 mm². The tensile bond strength values were 75, 74, 29, and 11 MPa for Si_3N_4/Al, sapphire/Al, Al_2O_3 (sintered)/Al, and AlN/Al. Failure of Si_3N_4/Al and sapphire/Al joints occurred within the aluminium adjacent to the interface in a ductile manner. Therefore it might be assumed that their fracture stress is mainly determined by the fracture stress of Al. However, Al/Al joints showed a much higher tensile strength of 175 MPa. This discrepancy can be attributed to a large mismatch of the elastic moduli of the metal and the ceramics which causes a stress concentration at the bonded interface and a reduction of bond strength. The metal side of the fracture surfaces of joints manufactured from sintered alumina and Al showed many particles

broken off from the alumina ceramic whereas AlN/Al joints fractured mainly within the ceramic. The importance of surface activation of the metal by sputter cleaning and ultra high vacuum bonding was demonstrated by experiments in which aluminium was not sputter-cleaned prior to UHV bonding to silicon nitride at room temperature. Manufacturing of joints was not possible indicating that an oxide film or other species at the Al surface will prevent bond formation.

3.3. *Metal*/Al_2O_3

Welding of Al_2O_3/Al/Al_2O_3 joints was performed at 600°C/50 MPa using ASTM F19 test pieces made from 99.5 wt% Al_2O_3 and interlayers 500 μm in thickness of 99.99 wt% Al.[61] The Al surfaces were abraded prior to bonding. The surfaces of the ceramic to be joined were used in two conditions; as received with a roughness $R_a=1.4$ μm and lapped with a roughness $R_a=0.4$ μm. After bonding the joints were heat-treated at 400°C/30 min followed by an annealing at 200°C/4 h. Initial tensile bond strength values of 3 to 7 MPa were measured for a bonding time of 1 min which did not depend on the surface roughness of the ceramic investigated. SEM observations indicated that the initial strength was caused by local bonding at sites where asperity peaks of the ceramic have indented the metal. The bond strength increased with bonding time at 600°C reaching values of about 20 MPa after 40 min for the ground alumina surfaces and 32 MPa after 20 min for the lapped surfaces. The bonded area grew by a temperature activated process. A mean maximum bond strength of 50 MPa was obtained for joints welded at temperatures above the melting point of aluminium. To model diffusion bonding it was assumed that all the deformation occurred in the aluminium. The model considered the interfacial contact to occur in two stages; the indentation of a conical punch and the collapse of a symmetrical void. Techniques of Johnson[77] for the self indentation of spheres and Wilkinson and Ashby[78] for pore collapse in sintering were applied to solve the diffusion equations at the interface. The predictions of the model showed that the fraction of contact area is about 0.6 for lapped ceramic surfaces and about 0.2 for ground ceramic surfaces after 10 min at 600°C/50 MPa. The corresponding highest tensile strength values were 20 and 12 MPa. According to the model, the fraction of contact area will be 1 after about 1 h for lapped surfaces and after about 90 min for ground surfaces. If a proportionality between bond strength and contact area is assumed the predicted values will be in a reasonable agreement for joints manufactured from lapped ceramic specimens as can be seen by comparing the fractions of bonded area and strength. The obtainable maximum tensile strength was 38 MPa after 1 h bonding time. However, the maximum fracture strength of joints manufactured from ground ceramic specimens was only 26 MPa after 90 min bonding time indicating that a reduction in strength might be induced by flaws introduced in the ceramic during surface machining which were not healed up during the annealing treatment.

The ion vapour deposition (IVD) method, direct diffusion bonding and the application of metal interlayers were applied in a study on metal/alumina bonding.[79] Polished alumina pieces of 99.7 wt % Al_2O_3 of dimensions 20 mm·17 mm·16 mm, 99.9 wt% Nb sheets of 2 mm thickness and interlayers of 50 and 125 μm thickness of the metals Ni (99.0 wt%), Zr (99.8 wt%), and Hf (97 wt%) were used for the bonding experiments. They were stacked to sandwich-like configurations of the sequence Al_2O_3/metal/Nb/metal/Al_2O_3 and Al_2O_3/Nb/Al_2O_3. Diffusion bonding was carried out in a high vacuum chamber under a mechanical pressure of 6 to 10 MPa. The specimens were held for 2 or 1 h at the bonding temperature and indirectly heated by an induction coil *via* a Mo susceptor. The highest fracture resistance values K_C of 4.7 MPa·m$^{1/2}$ were measured for Nb/Al_2O_3 joints with Ni interlayers of 50 μm thickness bonded at 1 200°C/2 h. Fracture occurred within the ceramic. For comparison the fracture resistance K_C of Nb/Al_2O_3 joints with reactive Zr interlayers was only 1.1 MPa·m$^{1/2}$ after bonding at 1 650°C/2 h and Nb/Al_2O_3 joints with Hf interlayers bonded at 1 800 °C/1 h fractured already during cutting of the bend test specimens. It might be assumed that the strong reaction between Zr or Hf and alumina leading to the formation of ZrO_2 or HfO_2 at the metal/ceramic interface and to the uptake of Al into the metal caused cracking in the adjacent alumina ceramic and the observed degradation of bond strength. The beneficial effect of Ni interlayers which enables excellent bonding at relatively low welding temperatures is thought to be due to an intimate interfacial contact between metal and ceramic achieved by plastic deformation of these interlayers. Experiments of direct bonding and IVD assisted diffusion bonding of Al_2O_3/Nb/Al_2O_3 joints showed that the bonding temperature could be reduced appreciably without any loss in bond strength by IVD preparation of the ceramic surfaces. Alumina pieces were coated by IVD technique with a 2 μm Nb layer. The Nb ions penetrated about 0.5 μm into the alumina prior to bonding. Interfacial fracture was observed for directly bonded joints whereas joints prepared from IVD coated alumina fractured within the Nb IVD coating adjacent to the alumina. The fracture resistance of the latter joints was 4.0 MPa·m$^{1/2}$ after welding at 1 500°C/1 h/6 MPa whereas K_C values of directly bonded joints were 3.1 and 3.7 MPa·m$^{1/2}$ after welding at 1 500°C/2 h/10 MPa and 1 700°C/2 h/10 MPa, respectively. The corresponding bond strength values of the directly bonded joints were 268 and 200 MPa, respectively, measured in four-point bend tests.

The finite element method was applied to select suitable interlayer materials for optimum diffusion bonding of metal/ceramic combinations with thermal expansion mismatches.[80] A butt joint of 5 mm in diameter was chosen consisting of a ferritic steel and an Al_2O_3 cylinder of 2.5 mm height bonded by an interlayer material of variable thickness between 0.2 and 2 mm. The interlayer consisted of Nb, Mo, Ti,

or an Al_2O_3–50vol%Fe cermet. A temperature difference of 975 K was used for the calculations which were performed under the assumption that the materials behave elastically without any plastic deformation. Since plastic deformation will relieve stress concentrations within the ceramic part it was expected that the calculations would over-estimate the internal stresses. The results demonstrated that the maximum tensile stress decreased with increasing interlayer thickness. Nb was most effective in reducing internal stresses because it has the same thermal expansion coefficient as alumina. Bonding experiments were performed at 1 300°C/100 MPa/30 min to join Al_2O_3 to a Nb interlayer of 1 mm thickness or to a double 0.5 mm Nb/0.5 mm Mo interlayer. To avoid formation of intermetallic compounds the bonded pieces were welded in a second step at 1 000°C/100 MPa/30 min to steel. The tensile strength of the steel/Nb/Al_2O_3 joint was only 5.6 MPa whereas that of the steel/Mo/Nb/Al_2O_3 joint was 63 MPa. The increase in strength and the decrease in residual tensile stresses in Al_2O_3 by the introduction of an additional Mo interlayer were explained by a reduction in shrinkage of Nb at the steel side caused by a smaller thermal expansion coefficient of Mo in comparison to Nb and steel. The calculated maximum tensile stresses in the ceramic were 400 and 300 MPa for a 1 mm Nb foil and a 0.5 mm/0.5 mm Mo/Nb double interlayer, respectively. The corresponding maximum internal stresses in the steel part were 650 and 1 400 MPa. After bonding the internal thermal stresses decreased substantially by plastic deformation of the metal part of the joint. The FEM model studies on the effect of interlayers demonstrated that the following relations between the thermal expansion coefficients α of the ceramic c, metal interlayers I and II, and metal m must be obbeyed to reduce residual stresses at the ceramic/metal interface[81]:

$$\alpha_c \approx \alpha_I < \alpha_m$$

for ceramic/interlayer I/metal joints .....(5)

$$\alpha_c \approx \alpha_I > \alpha_{II} < \alpha_m$$

for ceramic/interlayer I/interlayerII/ metal joints .....(6)

The application of soft metals of high plastic deformability as interlayer materials which are placed adjacent to the ceramic will increase the efficiency of thermal stress relief. Four-point bend test specimens cut from Al_2O_3/Nb/Mo/steel joints showed very high bond strength values of about 500 MPa. Thermal cycling between room temperature and 500°C up to 100 cycles did not have much influence on room temperature strength. It was argued that cutting and grinding the joints after bonding might increase bond strength by removal of defects and relief of residual stresses.

Alumina of 99.7 wt% purity was bonded to austenitic steel *via* a double Ti/Mo interlayer of 0.5 mm/0.5 mm thickness.[82] Al_2O_3 disks of 5 mm diameter and 1 mm thickness and steel pieces of the same diameter and 2.5 mm height were used. The tensile strength values of steel/Mo/Ti/Al_2O_3 joints bonded at 1 000°C/12 MPa/3 h in a vacuum of 10^{-4} mbar exceeded 60 MPa. Metallographic observation revealed that Ti_3Al or Ti_2Al was formed at the Al_2O_3/Ti interface. Fracture occurred at this interface. Some small fragments of alumina adhered to the Ti fracture surface.

Experiments were conducted to determine the optimum bonding conditions for alumina/stainless steel joints.[83] Samples of 10 mm high, 16 mm outer diameter, and 7 mm inner diameter of Fe–18wt%Cr–9wt%Ni–1wt%Ti stainless steel were used which were placed between 2 ASTM F19 test pieces fabricated from a 97.5 wt% Al_2O_3 ceramic. 0.5 mm thick Al annuli were inserted as interlayers between the ceramic and stainless steel pieces. Furthermore, truncated cone alumina samples were bonded *via* 1 mm Al foils to disks of Cu, Fe, Pt, Ti, and stainless steel. The tensile bond strength of stainless steel/alumina joints fabricated from ASTM test pieces was 42 MPa after welding at 625°C/50 MPa/30 min in an evacuated chamber. Failure occurred through an intermetallic layer of 19 μm thickness formed at the Al/steel interface. Further increasing the welding temperature promoted alumina/aluminium bonding but also accelerated the growth of the weakening intermetallic layer at the steel/aluminium interface. The data presented in this study also demonstrated the strengthening of Al/Al_2O_3 interfaces by low-temperature stress-relieving anneals. Experiments performed using truncated cone alumina specimens showed the detrimental effect of thermal expansion mismatch between alumina and metal. Bonding was produced at 550°C/50 MPa/30 min in an argon-filled chamber. The obtained results are given in Fig. 7. The tensile strength of these joints decreased steadily as the coefficient of thermal expansion exceeded the value of $7 \cdot 10^{-6}$ K^{-1} of alumina.

Studies on diffusion bonding of Ti, Ti–Ta alloys, Ti–Nb alloys to alumina for composite dental implants[84-88] were supplemented with experiments on Ti/Al_2O_3 joints using Al and Nb interlayers.[88] High vacuum bonding of 99.9 wt% Ti to alumina of 99.7

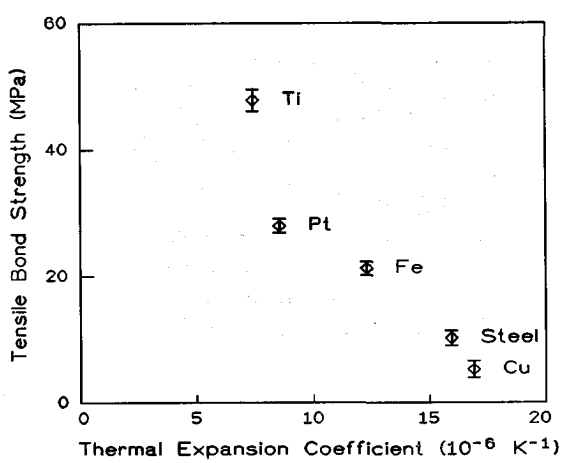

Fig. 7. Tensile strength of alumina–metal joints bonded with Al interlayers as a function of the metal thermal expansion coefficient.[83]

wt% impurity at 1 200°C/1 h led to crack formation within the ceramic starting at the bonded edges. The failure of these Ti/Al_2O_3 joints was caused by thermal expansion mismatch between both materials. TiO and $TiAl_3$ were formed at the metal/ceramic interface. To reduce thermal stresses induced into the joint during cooling from the welding temperature, Ti–30wt% Ta and Ti–40wt%Nb alloys of lower thermal expansion mismatch than pure Ti were chosen for the metal part of the joints. Optimum results were obtained after bonding at 1 200°C/4 MPa/1 h in a vacuum of 10^{-5} mbar for Al_2O_3/Ti–30Ta/Al_2O_3 joints fabricated from Ti alloy disks of 2 mm thickness and alumina pieces of 17 mm·17 mm·20 mm. They showed fracture energy values G_c of 38 ± 4 J/m^2 and fracture resistance values K_c of 2.4 ± 0.3 MPa·m$^{1/2}$ which were obtained in four-point bend tests using notched specimens of dimensions 2 mm·4 mm·40 mm. The fracture energy and fracture resistance values of Al_2O_3/Ti–40Nb/Al_2O_3 joints bonded at 1 400°C/4 MPa/1 h were 40 ± 13 J/m^2 and 2.6 ± 0.8 MPa·m$^{1/2}$. However, these joints were assumed to be less reliable because of the appreciably larger scatter of their bond strength data G_c and K_c and the high oxygen content in the metal part of more than 20 at% by which the Ti–40Nb alloy was severely embrittled. The oxygen content of the Ti–30Ta/Al_2O_3 joints was less than 10 at%. Failure of the joints occurred parallel to the interfaces within the ceramic which is typical for a strong metal/ceramic bond. The microstructure of the metal part of the Ti–30Ta/Al_2O_3 joints was refined by an additional annealing at 800°C/1 h. The metal part was subdivided into a reaction zone formed by TiAl and Ti_3Al, a transition zone consisting of plate-like α-Ti embedded in β-Ti, and the bulk Ti alloy which is characterized by a microstructure of acicular fine plates of α-Ti in β-Ti or transformed β-Ti. Experiments to join Ti to Al_2O_3 *via* 50 to 120 μm thick Al foils at bonding temperatures below the melting point of Al were not successful. The Al foils were strongly embrittled by the reaction with Ti. Very promising results were obtained with Nb interlayers of 10 μm thickness and 99.9 wt% purity. The Al_2O_3/Nb/Ti/Nb/Al_2O_3 joints were bonded at 1 500°C/4 MPa/1 h. After bonding the Nb interlayer had disappeared. A reaction layer containing TiAl and Ti_3Al was observed adjacent to the ceramic followed by a transition region enriched in Nb consisting of α-Ti and β-Ti. The fracture energy G_c of the Al_2O_3/Nb/Ti/Nb/Al_2O_3 joints was 40 ± 1 J/m^2 and the fracture resistance $K_c=2.72\pm0.07$ MPa·m$^{1/2}$.

Alumina ceramic bars of 25 mm length and 10 mm diameter were bonded to Ti or carbon steel bars of the same dimensions using a 0.6 mm aluminium interlayer cladded with two layers of an Al–10wt%Si layer of 40 μm thickness.[89] Welding was performed at 610°C/10 MPa/30 min in a vacuum of 3×10^{-4} mbar. The four-point bend strength values were 185 and 140 MPa for Al_2O_3/Ti and Al_2O_3/steel joints. Fracture occurred within the ceramic part. The lower strength of the Al_2O_3/steel joint was attributed to the larger thermal expansion mismatch of this combination.

Diffusion bonding of Cu to alumina was studied using 0.2 mm thick OFHC Cu disks and 8 mm thick 99.7 wt% Al_2O_3 ceramic disks both of 5 mm diameter.[90] Prior to bonding the Cu disks were polished and annealed in at 1 000°C/30 min in a vacuum of 10^{-3} mbar. Similarly, the bonding surfaces of alumina were finally polished with 1 μm diamond paste and annealed in air at 1 000°C/1 h. Optimum shear bond strength values of 50 MPa were obtained after bonding at 1 000°C/6 MPa/2 h in an Ar atmosphere. The mean roughness R_a of the ceramic surfaces of these Al_2O_3/Cu/Al_2O_3 joints was 0.3 μm. A distinct influence of the roughness of the alumina surface on the bond strength and the fracture behaviour of the joints was observed. High R_a values of 0.6 and 1 μm produced by grinding with diamond of grain size 40 and 150 μm, respectively, lead to low strength values of 20 and 15 MPa. The reduction in strength was caused by the introduction of flaws into the ceramic interface region and by pull-out of grains. Extensive void formation was found at the copper side of the interface fracture of joints manufactured from well-polished ($R_a=0.05$ μm) ceramic pieces. The effect was thought to be caused by gas evolution. TEM studies revealed that very small Cu_2O particles were dispersed in copper. Only a 0.1 μm layer of microcrystalline alumina but no reaction layer was detected at the metal/ceramic interface. In another set of experiments copper was preoxidized before bonding by annealing at 1 000°C in a low oxygen atmosphere to produce 0.7 and 2.2 μm Cu_2O layers on Cu.[91] Generally, the bond strength of preoxidized Cu was lower than that of nonoxidized Cu and decreased after a maximum at 1 or 2 h with increasing bonding time. Fractographic studies revealed the existence of 3 different bonding zones. The inner zone III contained $CuAlO_2$ at the interface after 2 h bonding time, after 6 h it disappeared and was substituted by a microcrystalline Al_2O_3 layer of about the same thickness. Zone III was under normal compression stress during bonding. The middle zone II is a zone of adhesion. It had an annular shape. The copper was plastically deformed during welding in this region of high shear stresses. The outer zone I not subjected to high stresses during bonding showed variable adhesion and was in contact with the furnace atmosphere. $CuAlO_2$ which was formed at the beginning of the bonding treatment was destabilized in favour of Al_2O_3 and Cu_2O by diffusion of oxygen. This was correlated to the observed decrease in bond strength.

Cu/Al_2O_3 joints were studied with respect to their fracture toughness and the influence of the bonded area and interfacial impurities on the bonding behaviour. Al_2O_3/Cu/Al_2O_3 joints were fabricated from an alumina ceramic of grain size 18 μm (mean intercept length) cut to the dimensions 11·6·1.5 mm^3 containing 300 wt. ppm Mg, 25 ppm K, 20 ppm Na, and 6 ppm Ca and high purity 30 μm thick polycrystalline Cu foils containing 20 wt. ppm Ag as the main impurity.[75] Bonding was carried out in the temperature range 850 to 1 050 °C for 10 min under a

mechanical pressure of 20 MPa. The bonding atmosphere was a purified gas mixture of 25/75 vol% H_2/N_2 which contained less than 1 vol. ppm H_2O. The fracture toughness of the joints was determined by double cantilever beam (DCB) tests. The obtained fracture toughness data K_{Ic} were 1.9, 3.7, 4.3, 4.2, and 4.5 MPa·m$^{1/2}$ for joints bonded at 850, 900, 950, 1 000, and 1 050°C, respectively. The fracture toughness of the alumina ceramic was 3.2 MPa·m$^{1/2}$. The observed dependence of the interfacial fracture toughness on the bonding temperature could not be completely accounted for by the temperature dependence of the amount of truly bonded interface area. Impurities found at the bonded interface by Rutherford backscattering spectrometry and Auger electron spectroscopy were Mo, Ca, C, S, and Cl all present in small amount. Their influence on the fracture toughness of the interface is as yet unknown. On the copper surfaces nearly no oxygen was present.

Experiments were performed to join alumina ceramics by a Cu–4wt%Ti alloy using 5 mm thick ceramic disks of 15 mm diameter and 0.6 mm thick metal disks of 6 mm diameter.[92] Optimum bonding was obtained after welding of sandwich-like configurations ceramic/metal/ceramic at 800°C/20 min/50 MPa in a vacuum of $7\cdot10^{-5}$ mbar. The tensile bond strength was 45 MPa for a joint fabricated from a 99.6 wt% alumina and Cu–4wt%Ti. The bond strength of Al_2O_3/Cu/Al_2O_3 joint was only 20 MPa. As with active metal brazing Ti was enriched at the interface due to the redox reaction between metal and ceramic.

Alumina ceramic was bonded to Ti with and without intermediate TiH_2 layers.[93] The materials used in this study were 5 mm thick discs of commercially pure Ti of 15 mm diameter, 8 mm thick discs of 99.6 wt% Al_2O_3 ceramic of 15 mm diameter and TiH_2 powder of 325 mesh. Al_2O_3/Ti/Al_2O_3 joint configurations with TiH_2 interlayers were heated in a vacuum chamber which was evacuated to a pressure of $7\cdot10^{-5}$ mbar. At 200°C the organic constituents of the powder interlayers evaporated. Further heating leads to the decomposition of TiH_2 which started at about 400°C. Bonding was performed at 850°C/62 MPa and 900/40 MPa for 10 min to 1 h. Maximum bond strength values measured in four-point bend tests were 126 MPa after bonding at 900°C/30 min using TiH_2 interlayers and 105 MPa after direct bonding of Ti and Al_2O_3 at 900°C/40 min. The obtained slight difference in strength was attributed to a better filling up of pores and voids at the ceramic interface by powder particles of the TiH_2 interlayer. $AlTi_2$, Ti, and Al_2O_3 were found by X-ray diffraction at the fracture surface of joints manufactured by the TiH_2 interlayer method.

Joints between 1.5 mm slices of polycrystalline Ni of 99.94 wt% purity and sapphire single crystal have been produced.[94] Diffusion bonding of stacks consisting of Al_2O_3/Ni/Al_2O_3 with the basal planes of sapphire as bonding surfaces was performed at 1 390 °C/4 MPa/2 h in a vacuum of 10^{-5} mbar. An intermediate spinel phase was found at the metal/ceramic interface. SEM observations revealed that a layer of about 1 μm thickness had been formed over the entire area of the diffusion bond. The spinel phase had a crystallographic relationship with sapphire such that the closed-packed planes and the closed-packed directions of the anion lattices were nearly parallel. The $NiAl_2O_4$ layer was composed of elongated subgrains which contained growth defects. The thermal expansion mismatch between the spinel phase and sapphire is very low. Despite the large difference between the thermal expansion coefficients of Ni ($13.3\cdot10^{-6}$ K^{-1}) and $NiAl_2O_4$ ($8\cdot10^{-6}$ K^{-1}) no evidence of deformation of the Ni metal was detected in TEM investigations. Further experimental and thermochemical studies showed that the formation of nickel aluminate spinel by solid state reaction between Ni and α-Al_2O_3 requires a certain oxygen activity which is less than that of the Ni–NiO equilibrium.[95] Using a sandwich-like stack of Ni/sapphire (0001)/Ni the assemblage consisting of 1 mm disks of 30 mm diameter was high vacuum welded between 2 sintered alumina blocks at 1 390°C/4 MPa/2 h. Prior to bonding, one of the polycrystalline Ni disks was hydrogen degassed to remove essentially all oxygen from solid solution, and the other was charged with about 670 at. ppm oxygen by annealing in NiO powder. Both pretreatments were conducted at 1 100°C/24 h. Light optical and TEM observations revealed the absence of any reaction layer at the oxygen-free Ni/Al_2O_3 interface and the formation of a spinel reaction layer about 1.5 μm thick at the oxygen-containing Ni/Al_2O_3 interface. This interface region showed also a light blue discolouration characteristic of Ni aluminate spinel. According to thermochemical studies and available data the reaction between oxygen-containing Ni and alumina can be described by the equation:

$$\mathrm{Ni}+[\mathrm{O}]_{\mathrm{Ni}}+(1+x)\,\mathrm{Al_2O_3}=\mathrm{NiO}\cdot(1+x)\,\mathrm{Al_2O_3} \quad \text{.....(7)}$$

where $[O]_{Ni}$ denotes oxygen dissolved in solid Ni and x varies between 0 and 0.38 at 1 390°C indicating that Ni aluminate is nonstoichiometric with considerable solubility for Al_2O_3. From the standard free energy of the reaction the equilibrium oxygen activity in solid Ni can be derived as a function of temperature:

$$a_{[\mathrm{O}]_{\mathrm{Ni}}}=\exp\left(-7\,230/T+0.53\right) \quad \text{.....(8)}$$

where $a_{[O]_{Ni}}$ is given in at% oxygen in nickel.
Oxygen activities above the equilibrium activity will lead to spinel formation wheras below this threshold activity oxygen-containing Ni will be in equilibrium with Al_2O_3. Furthermore, the equilibrium activity of oxygen at the bonding temperature of 1 390°C is 220 at. ppm which confirms the experimental results that the threshold is less than 670 at. ppm oxygen.

Alumina ceramic containing 91 wt% Al_2O_3 and 7 wt% SiO_2 was bonded to a Ti–6Al–4V alloy according to the following procedure.[96] The surface of the ceramic was coated with Ti powder and annealed at 1 100°C/1 h in a vacuum of $5\cdot10^{-5}$ mbar. After removing of unreacted powder a 99.5 wt% Ni

foil of 60 μm thickness was inserted between the alloy and the pretreated alumina. Metal disks of 20 mm diameter and 3 mm thickness with a central hole of 6 mm diameter for tensile testing of the joints were used for the experiments. The ceramic parts were 5 mm thick disks of 12.7 mm diameter. Optimal bonding occurred after welding at 1 000°C/1.2 MPa/1 h. The tensile bond strength of 40 MPa determined at room temperature was maintained up to a testing temperature of 700°C. The joints fractured at the interface or within the ceramic. An intermediate two-phase layer of about 100 μm thickness was formed between the ceramic and the Ti alloy.

3.4. *Metal*/ZrO_2

Disks of dimensions 10 mm·10 mm·3 mm made from a 3 mol% yttria-stabilized zirconia ceramic and Pt foils of 1, 20, and 50 μm thickness were used to produce ZrO_2/Pt/ZrO_2 joints.[97] Prior to bonding the zirconia disks and Pt foils were annealed at 1 000°C/2 h in an oxygen atmosphere. Diffusion bonding of the joints was performed at 1 500°C/0.15 MPa/4 h in air or in an oxygen atmosphere. The maximum shear strength of joints with 20 μm Pt interlayer foils was 134 MPa and that of joints with 50 μm Pt foils was 143 MPa. The joints fractured at the metal/ceramic interface. X-ray photoelectron spectroscopy studies indicated the formation of an interfacial Y-containing Pt–Zr–O compound. However, only monoclinic zirconia was detected at the interface by thin film X-ray diffraction.

Diffusion bonds were manufactured from polished TZP zirconia bars of 10 mm square section and 15 mm length and thin foils of Pd 100 μm in thickness. ZrO_2/Pd/ZrO_2 joints were bonded at 1 050 and 1 100 °C in a vacuum of 10^{-4} mbar for various times and cut into bars of 3 mm square section for four-point bend tests or into double torsion fracture toughness specimen.[98] The bond strength increased with increasing bonding time and was larger after bonding at 1 100°C. A maximum bond strength of 350 MPa was obtained after welding at 1 100°C/10 MPa/2 h. The fracture toughness G_c underwent a rapid change after about 30 min bonding time at both temperatures from $G_c<80$ J/m² to G_c values of 200 J/m² for the 1 050°C joints and 300 J/m² for the 1 100°C joints. This change is accompanied by a dramatic change in fracture surface behaviour with a transition from a smooth appearance to a rough surface showing extensive plastic deformation. Joints of high fracture toughness showed a grey discolouration of zirconia adjacent to the interface. To explain this behaviour an effect of the oxygen stoichiometry of zirconia on interfacial adhesion was assumed. Optimum stoichiometry was thought to be obtained in a vacuum of 10^{-4} mbar at some temperature above 1 000°C after some critical time and to be accompanied by a high adhesive strength sufficient to enable ductile tearing of the palladium near the interface. This assumption was supported by the fact that good joints lost their strength after annealing in air at 1 050°C/2 h.

Ceramic/metal/ceramic joints were manufactured from PSZ zirconia blocks of the dimensions 20 mm·17 mm·16 mm (thickness) and from Al or Al alloy plates of 2 mm thickness.[99] The compositions of the metals were 99.99 wt% Al, Al–2wt%Li, Al–6Cu, Al–6Cu–1Li, and Al–6Cu–2Li. Bonding was performed at 620°C/4 MPa/40 min in a high vacuum. From the bonded joints four-point bend test specimens of 2 mm width, 3 mm thickness, and 32 mm length were cut. Maximum bond strength values of 280 to 360 MPa were obtained for joints with an Al–6Cu–2Li interlayer which is in the α+liquid phase state at the bonding temperature. For Al–6Cu–2Li/PSZ joints fracture was initiated at the interface and continued to propagate within the ceramic parallel to the interface. The bond strength of the Al/PSZ joints welded under solid-state conditions was only about 20 MPa. The high bond strength of the Al–6Cu–2Li/PSZ joints was attributed to the high ductility of the alloy which showed a fracture elongation of 24 %. The bond strength values of joints manufactured with interlayers of the other alloys also partially melted during the welding operation were only 55, 200, and 190 MPa and the corresponding fracture elongations of the Al–2Li, Al–6Cu, and Al–6Cu–1Li alloys were 2.4, 15, and 7.8 %, respectively. A black zirconia layer of about 300 μm was formed at the metal/ceramic interfaces caused by the redox reaction between Al and ZrO_2.

3.5. *Metal*/MgO

Reaction welding studies were performed to join 2 pieces of 99.7 wt% MgO magnesia ceramic of dimensions 7 mm·10 mm·20 mm using Ni foils of 10 or 50 μm thickness as interlayers at 1 300 and 1 600°C in air.[100] The dimensions of the surfaces to be bonded were 7 mm·10 mm. During long time and high temperature exposure the Ni foils were transformed to a NiO–MgO solid solution forming a continuous interfacial transition layer between the magnesia blocks. A maximum bend strength of 63 MPa was obtained for a MgO/NiO–MgO/MgO joint reaction welded at 1 600°C/64 h. The fracture strength of the magnesia ceramic annealed for 64 h at 1 600°C was 90 MPa whereas the strength of the as-received magnesia ceramic was 140 MPa.

3.6. *Metal*/Si_3N_4

The preparation of Mo/Si_3N_4 joints is difficult because of the thermal expansion mismatch between silicon nitride and Mo which will induce residual stresses during manufacturing and reduce bond strength. In order to relieve these stresses ductile nickel was used as an insert metal.[101] Discs of pressureless sintered silicon nitride of 15 mm diameter and 10 mm thickness containing less than 5 wt% oxide additives were bonded to Mo discs of the same dimensions at temperatures between 900 and 1 200°C using Ni sheets of 0.6 mm as insert metals. A maximum shear strength of 85 MPa was obtained for specimens bonded at 1 000°C/1 h/9.8 MPa in a vacuum of about 10^{-5} mbar. *In-situ* light optical studies of the bonding process showed that a melt-like region

of about 2 μm thickness was formed at the ceramic/metal interface adjacent to a region in the bulk Ni which contains voids. This void region was considered to be the original interface. AES measurements revealed that Si and N from the decomposing silicon nitride diffused towards the Ni side forming a zone 2 μm thick of Ni alloy with presumably both elements in solid solution. TEM studies and X-ray diffraction experiments confirmed that no silicides or nitrides had been formed. The occurrence of the melt-like interface region was assumed to be due to a simple solid-state reaction between Si_3N_4 and Ni which lead to the formation of a Ni–Si–N solid solution.

High resolution electron microscopy, analytical electron microscopy, and microarea electron diffraction were combined in a structural analysis of the Si_3N_4/Ni interface.[102] Local formation of an amorphous phase, presumably SiO_2 or free Si was observed at some interface sites. However, diffraction patterns obtained by means of a microbeam of 30 nm in diameter only revealed the presence of Ni and Si_3N_4. Microbeam energy dispersive analysis confirmed that the Si content decreased with increasing distance from the interface. Mg and Al from the grain boundary of the ceramic did not take part in the diffusion towards Ni.

Interlayers consisting of aluminium cladded by 40 μm thick Al–10wt%Si layers were used to join a silicon nitride ceramic of fracture toughness $K_{Ic}=5.0$ MPa·m$^{1/2}$ to WC–Co cemented carbide, Kovar alloy and carbon steel at 610°C/10 MPa/30 min in a vacuum of $3\cdot10^{-4}$ mbar.[89] The interlayer thickness was 0.6 mm. The length of the Si_3N_4 and metal parts was 25 mm and their diameter 10 mm. The room temperature strength of the joints measured in four-point bend tests decreased with increasing difference in the thermal expansion coefficients of metal and ceramic due to induced residual stresses from 210 MPa for Si_3N_4/WC–Co and 175 MPa for Si_3N_4/Kovar to 56 MPa for Si_3N_4/steel. Fracture occurred within the ceramic part of the joints. The bond strength of Si_3N_4/WC–Co joints with Al–Si interlayers remained constant up to a test temperature of 300°C. At 400°C the bond strength was only 107 MPa. A maximum room-temperature bond strength of 230 MPa was achieved for Si_3N_4/WC–Co joints with a Al–Si interlayer of 1.2 mm thickness. Similar experiments performed with a sialon ceramic of fracture toughness $K_{Ic}=7.8$ MPa·m$^{1/2}$ showed a strength of 318 MPa for a sialon/WC–Co joint with 0.6 mm Al–Si interlayer bonded at 610°C/10 MPa/30 min. The strength values of sialon/WC–Co joints with 0.6 mm Fe–Ni–Cr or Fe–Ni–Co interlayers manufactured at 1 100°C/30 MPa/3 h were about 150 MPa and thus appreciably lower than those of the same metal/ceramic combination with Al–Si interlayers. Reaction products formed at the interface were assumed to reduce their bond strength.

A special bonding technique using an interdiffusing metals layer was applied to obtain silicon nitride joints of high bond strength.[103] This multilayer is composed of interface metal foils or films and an adjacent metal consisting of bulk material, sheet or thin film. During the bonding process the adjacent metal diffused into and through the interface metal to the metal/ceramic interface and reacts with the ceramic or intensifies the reaction. Blocks of Si_3N_4 containing alumina and yttria additives of dimensions 10 mm·14 mm·17 mm and 99.9 wt% Ni and 99.9 wt% Nb foil and sheet were used in this study. Bonding was performed at 950°C/20 MPa in a vacuum of 5×10^{-6} mbar. The bonding time varied between 45 min and 6 h. From each bonded joint 4 four-point bend specimens were cut to determine the bond strength. A comparatively very high bond strength value of 290 MPa was obtained for a Si_3N_4/Ni/Nb/Ni/Si_3N_4 joint after a bonding time of 1.5 h. The thickness of the Nb layer was 1 mm and that of the Ni interface layers 10 μm. A Si_3N_4/Nb/Ni/Nb/Si_3N_4 joint manufactured under the same bonding conditions showed a bond strength of 180 MPa. The interdiffusing metals layer consisted of a 1 mm Ni layer enclosed by two 12.5 μm Nb interface layers. However, no bonding could be achieved for couples of Si_3N_4/Nb/Si_3N_4 and Si_3N_4/Ni/Si_3N_4 without interface layers of Ni or Nb, respectively. Electron probe microanalysis demonstrated that the adjacent metal has diffused during the bonding process through the interface metal to the metal/ceramic interface. The reason why the interdiffusing adjacent metal plays such an important role was not clarified. It might be assumed that it will confine the formation of reaction products to a narrow zone thus avoiding an embrittlement of the interface region. Well bonded Si_3N_4 joints were also obtained for a Ni(10 μm)/Cu(1 mm)/Ni(10 μm) interdiffusing metals layer.

The extent of reaction between Si_3N_4 and Ni–Cr alloys at temperatures between 1 000 and 1 200°C under argon depended strongly on the Cr content of the alloy and was maximum for a Ni–7wt%Cr alloy.[104] Y_2O_3 and Al_2O_3 additives in silicon nitride lead to a loss of adherence due to segregation of these additives at the metal/ceramic interface.

In another series of experiments silicon nitride and an Fe–26wt%Cr alloy was bonded in Ar using a Ti foil of 20 μm thickness and Ni sheet of 1 mm thickness as interlayers. The bond strength of the Fe–Cr/Ni/Ti/Si_3N_4/Ti/Ni/Fe–Cr joints obtained in bending tests was 70 MPa after diffusion bonding at 1 150°C/1 h.[105] Welded joints showed strength values which decreased at first to 40 MPa when annealed at 1 100°C for 10 h and then increased to 80 MPa after annealing for 100 h at the same temperature. The interface region can be subdivided into 2 layers. The layer adjacent to the ceramic consisted of TiN, Ti(Si, Ni) and oxides of the ceramic additives. The second layer is composed of TiNi, $TiNi_3$ and Ni–Ti solid solution. During high-temperature annealing TiNi decomposed to $TiNi_3$ and then to a Ni–Ti solid solution. A considerable increase in bond strength was observed when the thickness of the TiNi layer was reduced to a few micrometers. At annealing temperatures the thickness of the TiN layer increased

leading to a low bond strength or even failure of the joint during cooling. According to the microstructural observations it was assumed that the formation of an interfacial TiN layer is not a necessary prerequisite for bonding.

Pressureless sintered silicon nitride was bonded to 0.45 wt% steel using hot isostatic pressing (HIP) in a glass cell.[106] The temperature and pressure ranges were 1 000 to 1 220°C and 50 to 100 MPa, respectively at a bonding time of 30 min for specimens consisting of two 10 mm·10 mm·15 mm ceramic blocks with an intermediate steel sheet. During the HIP cycles Ar gas pressure was applied at temperatures above 800°C. High bond strength values of 600 MPa were obtained for Si_3N_4/steel/Si_3N_4 joints fabricated at 1 200°C/100 MPa/30 min at testing temperature between room temperature and 600°C using four- and three-point bend testings. After bonding the thickness of the steel layer was 0.35 mm. At a testing temperature of 700°C the fracture strength was reduced to about 280 MPa. However, the room temperature bond strength decreased considerably when the thickness of the steel layer was increased to 0.8 or 1.8 mm. The corresponding values were 285 and 20 MPa. Visible cracks were formed in silicon nitride parts of the joints for steel layer thicknesses of more than 1 mm due to thermal expansion mismatch between metal and ceramic. W interlayers between silicon nitride and steel were recommended to reduce residual thermal stresses.

A finite element method was used to calculate the effects of the thickness of the silicon nitride part on residual stress in a silicon nitride/steel joint under the assumption of fully elastic media.[107] These effects were also studied experimentally by tensile test of isostatically hot-pressed joints. It was shown that the maximum residual stress in silicon nitride increased with increasing thickness of the silicon nitride part of the bimaterial joint. In a Si_3N_4/steel joint of 10 mm in diameter with a 10 mm thick steel part the calculated maximum stress was 400 GPa for a silicon nitride part of 1 mm thickness. The maximum stress reached a plateau value of about 1 400 MPa for silicon nitride parts which are thicker than 5 mm. The assumed difference between bonding and room temperature was −975 K. The diameter of the joints in the bonding experiments was 7 mm and the thickness of silicon nitride ranged between 0.1 and 1 mm. 3 mm thick steel disks were used. Isostatic hot pressing of Si_3N_4 joints was carried out at 1 200°C/100 MPa/30 min.[81] The obtained tensile bond strength decreased from about 50 MPa for a 0.1 mm silicon nitride layer to 9 MPa for a 0.5 mm and 6 MPa for a 1 mm layer thus confirming that the thickness effect was caused by thermal expansion mismatch between the bonded materials. All joints fractured within the ceramic which indicated also the presence of large residual stresses.

3.7. *Metal*/AlN

AlN/Mo/AlN joints were manufactured by diffusion bonding at 1 200°C/7 MPa in a vacuum of about 10^{-5} mbar from AlN blocks of dimensions 20 mm·20 mm·20 mm and Mo sheets of 2 mm·20 mm·20 mm.[108] The thermal expansion mismatch between these materials is small. Prior to joining the AlN surface was precoated with Ti using ion implantation with 20 keV N ions and Ti vapour deposition. The Ti implantation depth of AlN was about 10 nm. Additionally, Ti was deposited onto Mo by a normal evaporation technique. Bend test specimens of 2 mm width, 3 mm thickness and 30 mm length were cut from the bonded joints. Room temperature bond strength values of 115 MPa were measured for joints with a Ti interlayer thickness of 4.5 μm whereas the strength of the bulk AlN ceramic was 400 MPa. Fracture occurred at the AlN/Ti interface. It is interesting to note that the bond strength of these joints was only reduced to 83 MPa at a testing temperature of 800°C. The obtained rather low bond strength values were assumed to be caused by the formation of TiN containing Al at the AlN/Ti interface. However, AlN/Mo/AlN joints diffusion bonded at 1 200°C by means of Ti filler metal layers of 9 μm thickness without prior ion implantation treatment fractured already during the cutting operation indicating that Ti implantation into the AlN lattice is essential to achieve bonding.

3.8. *Metal*/SiC

The reactions between SiC powder and powders of Ti, Cr, Fe, or Ni were studied.[109] After mixing in a metal/ceramic volume ratio of 3: 7 the powder mixtures were compacted under a hydraulic pressure of 45 MPa and heated in 99.9 % Ar gas containing 10 ppm O_2 and 80 ppm N_2 in the range 600 to 1 300°C for 5 to 100 h. X-ray diffraction analysis of SiC/Ti mixtures showed that TiC and Ti_5Si_3 were formed at 850°C/5 h. An increase in the lattice parameter of Ti_5Si_3 was observed after annealing at 900°C for 5 to 100 h which is probably due to the uptake of carbon. The composition of titanium carbide TiC_{1-x} is hypostoichiometric with $0<x<0.5$ for specimen heated at 850°C for 5 h. Cr_3Si and Cr_7C_3 were analysed in SiC/Cr mixtures only after annealing at 900°C for 66 h. The silicide was adjacent to SiC and the carbide near the metal indicating that C could diffuse further than Si because of the lesser stability of carbide. In the Fe/SiC system, metal rich Fe_2Si containing carbon was found in the reaction zone of the metal and graphite flake were present in SiC. δ-Ni_2Si was detected in Ni/SiC mixtures heated at 900°C for 5 h. After heating at 1 000°C/5 h Ni_5Si, Ni_3Si, and $Ni_{31}Si_{12}$ were identified by X-ray diffraction. Graphite was finely dispersed in Ni_2Si after annealing at 900°C for 5 h. In the Fe and Ni systems carbide formation was not observed.

The interactions of dense α-SiC with Ni and Fe have been investigated at 850°C.[110] The experiments were performed with 99.95 wt% Fe, 99.99 wt% Ni, and hot-pressed SiC of purity 99.5 wt% SiC pieces of 3.5 mm·4.8 mm·5.0 mm and metal disks of 9 mm in diameter and 5 mm thickness were stacked to a Ni/SiC/Fe sandwich and annealed under a pressure

of 13 MPa in a vacuum of 10^{-6} mbar for 20 h. Alternating interlayers of Ni_2Si and Ni_2Si with free carbon, alternating layers of Ni_5Si_2 and Ni_5Si_2 with free carbon, and a layer of Ni_3Si were observed in the SiC–Ni system by microprobe analysis whereas in the SiC–Fe system precipitates of carbon were found in a Fe–Si alloy interlayer. The metal/ceramic interface was marked with alumina particles of 5 μm diameter. The marker experiments showed that Ni and Fe migrated whereas Si and C were immobile.

Bonding of α-SiC to α-SiC using interlayers of the metals Cu, Pd, Ti, and Hf of a purity of better than 99.9 wt% was studied.[57] After cleaning by Ar ion bombardment the SiC surfaces were coated with 0.2 to 3 μm metal layers by sputtering. The coated ceramic specimens were annealed in Ar at temperatures between 600 and 1 700°C to investigate the formation of reaction products and to evaluate the adherence of the coatings by a scratch test. SiC/Ti/SiC joints were diffusion bonded at 1 450°C/30 MPa/1 h using 1 μm Ti interlayers. Pd films agglomerated at 800°C and formed Pd_3Si and Pd_2Si phases at the SiC/Pd interface. Agglomeration of Cu films was also observed and C–stabilized Cu_7Si was found after a heat treatment between 950 and 1 084°C. Hf and Ti did not show any agglomeration effects after tempering but the adherence of Ti coatings on the substrate exceeded that of Hf layers. $TiC_{0.43}$ was found by X-ray diffraction after Ti/SiC reactions in the range 700 to 1 000°C. Titanium carbide and Ti_5Si_3 as well as $TiSi_2$ and Ti_3SiC_2, both in small quantities, were detected after annealing between 1 000 to 1 300°C. Reaction products after annealing at 1 300 to 1 500 °C were mainly Ti_3SiC_2 and smaller amounts of titanium carbide with a maximum C/Ti ratio of 0.8. The plasticity of Ti_3SiC_2 was assumed to reduce residual stresses due to thermal expansion mismatch which was confirmed by bond strength measurements using four-point bend test specimens of the dimensions 3.5 mm·4.5 mm·50 mm and by micrographs of their interface regions. The obtained bond strength was 286 MPa for the SiC/Ti(Ti_3SiC_2)/SiC joints welded at 1 450°C whereas the strength of the SiC bulk material was 303 MPa. The corresponding Weibull parameters m were 10 and 14.8, respectively. Interfacial pores of the ceramic were filled with Ti_3SiC_2 demonstrating its plastic deformability. 80 % of fracture occurred within the ceramic.

Foils of 99.5 wt% purity Ti, Al/Ti/Al, or 99.7 wt% purity Zr were used as interlayers to join pressureless sintered SiC pieces.[111] Disks of 5 mm thickness and 8 mm diameter for structural investigations and rectangular pieces for bond strength measurements were cut from rods of SiC containing several per cents of Al_2O_3. The SiC was of 4H type, including small amounts of 6H type. Small hexagonal plates of α-SiC single crystals were also used in bonding experiments. The thicknesses of the Ti and Zr foils were 20 μm and the thickness of the 98 wt% purity Al foil was 15 μm. SiC/Ti/SiC and SiC/Zr/SiC joints were bonded at 1 500°C/0.34 MPa/1 h for structure observations and at 1 500°C/0.56 MPa/1 h for bend tests. Bonding of SiC/Al/Ti/Al/SiC joints was performed at 1 000°C/1 h in an ambient atmosphere. Four-point bend specimens of dimensions 2 mm·5 mm·20 mm were cut from the bonded pieces. Ti reacted with pressureless-sintered SiC to produce a Ti_3SiC_2 phase. The composition of the Ti layer inserted between α-SiC single crystals was somewhat different after the 1 h annealing at 1 500°C. In addition to Ti_3SiC_2 small amounts of $Ti_5Si_3(C)$ and $TiSi_2$ phases were also detected by X-ray powder diffraction and EPMA line profile analysis. Electron diffraction patterns revealed a crystallographic relationship of (0001)SiC || (0001)Ti_3SiC_2 and $\{10\bar{1}0\}$SiC || $\{10\bar{1}0\}Ti_3SiC_2$ between SiC and Ti_3SiC_2. SiC/Al/Ti/Al/SiC joints showed a thin TiC layer and a residual Al layer between SiC and $TiAl_3(Si)$. The $TiAl_3(Si)$ phase contained fine Al_2O_3 particles. In the case of SiC/Zr/SiC joints a mixed structure of ZrSi and ZrC compounds was produced by the metal/ceramic reaction. Fine Al_2O_3 particles from auxiliary binder in the SiC were also found in the insert. The bond strength of SiC/Zr/SiC joints was only 17 MPa. However, SiC/Ti/SiC joints showed a maximum room temperature strength of about 300 MPa which decreased to about 250 MPa at 1000°C. Fracture occurred within the interlayer. The room temperature bond strength of SiC/Al/Ti/Al/SiC joints was about 160 MPa. A steep decrease of strength was observed at 600°C for these joints. The relatively high bond strength was attributed to the formation of Ti_3SiC_2 for Ti interlayers and to that of a TiC layer for Al/Ti/Al triple inserts. TiC had a good lattice matching with SiC. The low bond strength of Si/Zr/SiC joints was thought to be caused by the unsufficient lattice matching of ZrSi and ZrC which SiC.

A study of the reaction between silicon carbide and Ni was performed using hexagonal polytype 6H–SiC single crystals and Ni films of about 200 nm thickness sputtered onto the (0001) surface of the SiC crystals.[112] The specimens were annealed in a high vacuum of $7 \cdot 10^{-6}$ mbar at temperatures of 500, 600, 700, 800, and 900°C for 15 min and afterwards examined by X-ray diffraction and transmission electron microscopy. Informations of local chemical composition were obtained by combined energy dispersive X-ray analysis and analytical electron microscopy. At all temperatures studied SiC reacts with Ni to form Ni silicides. Carbide formation could not be detected. After annealing at 600°C the intermediate reaction phase consisted of grains of about 50 nm in size which are not always in contact with the SiC substrate. About 25 nm wide and 200 nm long voids occupying the interface region were observed in TEM studies which were assumed to be caused by the ion mill thinning operation. High resolution electron microscopy, electron diffraction patterns, and EDX analysis revealed that polycrystalline Ni_2Si and an amorphous phase, the latter probably by decomposition of SiC, were formed at the metal/ceramic interface. Localized formation of graphite or Ni carbide was not detected. The authors proposed the following mechanism for the SiC/Ni interfacial reaction.

SiC decomposes in vacuum at the annealing temperature and enriches in Si due to a fast diffusion of C towards the Ni side. Si forming the amorphous phase reacts with Ni to form silicides. Growth of some silicide grains leads to a direct contact with the SiC substrate at some sites of the interface so that a two-phase interlayer composed of Ni silicides and amorphous Si will be formed.

Reaction-sintered (RS) SiC containing 13 wt% free Si was bonded to Nb in a vacuum of $1.3 \cdot 10^{-4}$ mbar in the range of 1 100 to 1 500°C for 30 min to 6 h under a pressure of 0.5 to 2.0 MPa.[113] The dimensions of the ceramic and metal disks to be bonded were 6 mm in diameter and 4 mm in length. Maximum shear strength values of 87 and 85 MPa were measured for SiC/Nb/SiC joints produced at 1 400°C/2 MPa/30 min and 1 300°C/2 MPa/30 min. Fracture occurred at the metal/ceramic interface and partially within the ceramic. The fracture shear stress of joints bonded at 1 400°C decreased with increasing testing temperature to a value of about 50 MPa measured at 900°C. The interfacial phase Nb_5Si_3 was identified in joints bonded at 1 300°C/0.5 MPa/6 h by energy dispersive microanalysis. The reaction products Nb_5Si_3 and $NbSi_2$ were found after bonding of RS SiC, and Nb at 1 400°C/0.5 MPa/4 h. It was argued that the large amounts of free Si in RS SiC promoted the formation of silicides.

3.9. Interfacial Voids

Informations on the pressure and composition of residual gases in interfacial voids of diffusion bonded metal/metal joints are of interest for metal/ceramic joints. Oxygen free high conductivity copper, Al, Ti, stainless steel, and a Ti–6Al–4V alloy were used in welding experiments performed in vacua of 4×10^{-5}, 0.04 mbar, and in air, Ar and hydrogen of 10^3 mbar.[114] In metal/metal joints manufactured in Ar atmosphere Ar gas remained in voids formed at the welded interface and prevented the shrinkage of the voids. Reactive gases in the welding atmosphere which form compounds with the metals could not be detected in interfacial voids whereas gases which dissolve in the metals were found and show equilibrium partial pressures within the voids. Auger analysis showed that the surfaces of Cu specimens are covered with carbon. During bonding in an oxygen and hydrogen containing atmosphere interfacial voids were formed in Cu joints which contained CO_2 and CH_4.

4. Concluding Remarks

Chemical reactions between ceramics and metals during bonding were shown to have a dominant influence on the bond strength of joints. In particular, after bonding at high temperatures close to the melting point of one of the constituents interfacial reaction layers form and interdiffusion is extensive. Theoretical predictions of the morphology and the chemical composition of reaction layers are limited because of the paucity of both thermodynamic and diffusivity data. Nevertheless, some guidelines for an optimization of the interfacial regions of joints are available. For example, extensive reaction product formation lowers the bond strength, since the newly formed phase usually is brittle, contains flaws and has strain mismatch.

The insertion of metal foils of adequate thermal expansion behaviour as interlayers between the metal and the ceramic parts prior to bonding has been proved to be a powerful tool in reducing internal stresses due to thermal expansion mismatch and enhancing the bond strength. Metal interlayers can also be used to mitigate excessive chemical reactions at metal/ceramic interfaces as shown by studies using the interdiffusing metal layer technique.

Informations on the role of impurities in the bonding of metals to ceramics are scarce. However, it was demonstrated that a temperature-dependent threshold content of oxygen dissolved in nickel exist above which a spinel layer is formed between solid nickel and alumina and below which the metal is bonded directly to the ceramic. Further studies are needed to determine the influence of bulk and interfacial impurities on the bond strength of joints. Ultra high vacuum diffusion bonding of metals and ceramics of well-defined impurity content including surface doping of the materials to be bonded can be used for this purpose.

Attempts to investigate the thermal and mechanical fatigue behaviour of joints and to apply nondestructive testing methods are still in the early stages. A standardization of bend testing methods for conventional bond strength determination is urgently needed.

REFERENCES

1) G. Petzow, T. Suga, G. Elssner and M. Turwitt: Sintered Metal–Ceramic Composites, ed. by G. S. Upadhyaya, Elsevier, Amsterdam, (1984), 3.
2) J. T. Klomp: Joining of Ceramics, Glass and Metal, ed. by W. Kraft, DGM, Oberursel, (1989), 55.
3) H. F. Fischmeister, G. Elssner, B. Gibbesch and W. Mader: Proc. of MRS Int. Meeting on Advanced Materials, Vol. 8, Metal–Ceramic Joints, Mater. Res. Soc., Pittsburgh, PA, (1989), 227.
4) M. Rühle and A. G. Evans: *Mater. Sci. and Eng.*, **A107** (1989), 187.
5) R. E. Loehman and A. P. Tomsia: *Am. Ceram. Soc. Bull.*, **67** (1988), 375.
6) M. G. Nicholas: Joining of Ceramics, Glass and Metal, ed. by W. Kraft, DGM, Oberursel, (1989), 3.
7) M. G. Nicholas: Proc. of MRS Int. Meeting on Advanced Materials, Vol. 8, Metal–Ceramic Joints, ed. by M. Doyama *et al.*, MRS, Pittsburgh, PA, (1989), 49.
8) M. G. Nicholas: Designing Interfaces for Technological Applications, ed. by S. D. Peteves, Elsevier, London, (1989), 49.
9) G. Elssner: Designing Interfaces for Technological Applications, ed. by S. D. Peteves, Elsevier, London, (1989), 77.
10) J. T. Klomp: Designing Interfaces for Technological Applications, ed. by S. D. Peteves, Elsevier, London, (1989), 127.
11) M. Rühle and W. Mader: Designing Interfaces for Technological Applications, ed. by S. D. Peteves, Elsevier, London, (1989), 145.

12) A. M. Stoneham and P. W. Tasker: Designing Interfaces for Technological Applications, ed. by S. D. Peteves, Elsevier, London, (1989), 217.
13) H. F. Fischmeister: Ceramic Microstructures '86, ed. by J. A. Pask and A. G. Evans, Plenum Press, New York, (1987), 1.
14) J. T. Klomp: Ceramic Microstructures '86, ed. by J. A. Pask and A. G. Evans, Plenum Press, New York, (1987), 307.
15) J. A. Pask: *Am. Ceram. Soc. Bull.*, **66** (1987), 1587.
16) R. J. Bondley: *Electronics*, **20** (1947), 97.
17) D. M. Mattox and H. D. Smith: *Am. Ceram. Soc. Bull.*, **64** (1985), 1363.
18) M. G. Nicholas and D. A. Mortimer: *Mater. Sci. and Technol.*, **1** (1985), 657.
19) P. C. Barrett: UK Patent 891705, (1962).
20) General Electric Co.: UK Patent 1128228, (1968).
21) C. A. Clarke and R. D. Berry: UK Patent 1109108, (1968).
22) T. Iseki, T. Kameda and T. Maruyama: *J. Mater. Sci.*, **19** (1984), 1692.
23) M. G. Nicholas, T. M. Valentine and J. M. Waite: *J. Mater. Sci.*, **15** (1980), 2197.
24) A. J. Moorhead and H.-E. Kim: *Ceram. Eng. Sci. Proc.*, **10** (1989), 1854.
25) M. G. Nicholas: Ceramic-Metal Interfaces, Fundamentals of Diffusion Bonding, ed. by Y. Ishida, Elsevier, Amsterdam, (1987), 25.
26) Y. V. Naidich and V. S. Zhuravlev: Joining of Ceramics, Glass and Metal, ed. by W. Kraft, DGM, Oberursel, (1989), 17.
27) W. K. Armstrong, A.C.D. Chaklader and J. F. Clarke: *J. Am. Ceram. Soc.*, **45** (1962), 115.
28) Yu. Naidichi: *Prog. Surf. Membrane Sci.*, **14** (1981), 353.
29) J. E. McDonald and J. G. Eberhart: *Trans. Metall. Soc. AIME*, **233** (1965), 512.
30) M. Nicholas: *J. Mater. Sci.*, **3** (1968), 571.
31) R. M. Crispin and M. Nicholas: *J. Mater. Sci.*, **11** (1976), 17.
32) A.C.D. Chaklader, W. W. Gill and S. P. Mehrota: *Mater. Sci. Res.*, **14** (1981), 421.
33) A.C.D. Chaklader, A. M. Armstrong and S. K. Misra: *J. Am. Ceram. Soc.*, **51** (1968), 630.
34) J. F. Burgess, C. A. Neuberger, C. Flanagan and R. E. Moore: Advances in Joining Technology, ed. by J. J. Burke, Brook Hill Publ., Chestnut Hill, MA, (1975), 185.
35) A. J. Moorhead, H. M. Henson and T. J. Henson: Ceramic Microstructures '86, ed. by J. A. Pask and A. G. Evans, Plenum Press, New York, (1987), 949.
36) B. Wielage and D. Ashoff: Joining of Ceramics, Glass and Metal, ed. by W. Kraft, DGM, Oberursel, (1989), 385.
37) W. Weise, W. Malikowski and H. Krappitz: Joining of Ceramics, Glass and Metal, ed. by W. Kraft, DGM, Oberursel, (1989), 33.
38) D. O. Patten, M. L. Torti and P. O. Charreyron: *Ceram. Eng. Sci. Proc.*, **10** (1989), 1866.
39) A. J. Moorhead and P. F. Becher: *J. Mater. Sci.*, **22** (1987), 3297.
40) T. Iseki and M. G. Nicholas: *J. Mater. Sci.*, **14** (1979), 687.
41) M. Ito, N. Ishida and N. Kato: SAE Technical Paper Series 88074, (1988).
42) M. G. Nicholas, D. A. Mortimer, L. M. Jones and R. M. Crispin: Harwell Report R-12940, (1988).
43) M. G. Nicholas and L. M. Jones: "Wetting and Bonding Nitride Ceramics", paper presented at the meeting "Joining of Ceramics, Glass and Metal", Bad Nauheim, FRG, (1989), 8 pp.
44) S. Tanaka: Proc. of MRS Int. Meeting on Advanced Materials, Vol. 8, Metal-Ceramic Joints, MRS, Pittsburgh, PA, (1989), 91.
45) T. Sera, A. Nitta, I. Tsuchitori, N. Hara, M. Yoshino and T. Watanabe: Proc. of MRS Int. Meeting on Advanced Materials, Vol. 8, Metal-Ceramic Joints, MRS, Pittsburgh, PA, (1989), 41.
46) X. S. Ning, K. Suganuma, M. Morita and T. Okamoto: *Phil. Mag. Lett.*, **55** (1987), 93.
47) M. Morita, K. Suganuma and T. Okamoto: *J. Mater. Sci.*, **22** (1987), 2778.
48) K. Suganuma, T. Okamoto and M. Koizumi: *J. Mater. Sci. Lett.*, **4** (1985), 648.
49) M. Naka and I. Okamoto: Proc. of MRS International Meeting on Advanced Materials, Vol. 8, Metal-Ceramic Joints, MRS, Pittsburgh, PA, (1989), 61.
50) K. Suganuma, T. Okamoto and M. Koizumi: *J. Mater. Sci.*, **22** (1987), 2702.
51) K. Suganuma and T. Okamoto: Fundamentals of Diffusion Bonding, ed. by Y. Ishida, Elsevier, Amsterdam, (1987), 71.
52) K. Suganuma, T. Okamoto and M. Koizumi: *Advanced Ceram. Mater.*, **1** (1986), 356.
53) P. Batfalsky, J. Godziemba-Maliszewski and R. Lison: Joining of Ceramics, Glass and Metal, ed. by W. Kraft, DGM, Oberursel, (1989), 81.
54) T. Iseki, T. Yano and Y.-S. Chung: *J. Ceram. Soc. Jpn. Int. Ed.*, **97** (1989), 697.
55) T. Iseki and T. Yano: *Mater. Sci. Forum*, **34-36**, (1988), 421.
56) T. Yano, H. Suematsu and T. Iseki: *J. Mater. Sci.*, **23** (1988), 3362.
57) B. Gottselig, E. Gyarmati, A. Naoumidis and H. Nickel: Joining of Ceramics, Glass and Metal, ed. by W. Kraft, DGM, Oberursel, (1989), 191.
58) T. Iseki, T. Maruyama and T. Kameda: *Proc. Br. Ceram. Soc.*, **34** (1984), 241.
59) E. Lugscheider and M. Boretius: Joining of Ceramics, Glass and Metal, ed. by W. Kraft, DGM, Oberursel, (1989), 25.
60) T. Yano, N. Takada and T. Iseki: *J. Ceram. Soc. Jpn. Int. Ed.*, **95** (1987), 324.
61) B. Derby: Ceramic Microstructures '86, ed. by J. A. Pask and A. G. Evans, Plenum Press, New York, (1987), 319.
62) M. Backhaus-Ricoult: *Ber. Bunsenges. Phys. Chem.*, **90** (1986), 684.
63) M. Backhaus-Ricoult and H. Schmalzried: *Ber. Bunsenges. Phys. Chem.*, **89** (1985), 1323.
64) M. Turwitt, G. Elssner and G. Petzow: Proc. of Symp. on "Ceramic Microstructures '86: The Role of Interface", ed. by J. A. Pask, A. G. Evans, Plenum Press, (1988), 969.
65) M. Turwitt, G. Elssner and G. Petzow: *J. de Physique*, **46** (1985), C4-123.
66) T. Suga and G. Elssner: *J. de Physique*, **46** (1985), C4-657.
67) M. Florjancic, W. Mader, M. Rühle and M. Turwitt: *J. de Physique*, **46** (1985), C4-129.
68) S. Morozumi, M. Endo, M. Kikuchi and K. Hamajima: *J. Mater. Sci.*, **16** (1981), 2137.
69) Y. Ishida, J.-Y. Wang and T. Suga: Proc. of MRS Int. Meeting on Advanced Materials, Vol. 8, Metal-Ceramic Joints, MRS, Pittsburgh, (1989), 145.
70) K. Burger, W. Mader and M. Rühle: *Ultramicroscopy*, **22** (1987), 1.
71) M. Rühle, M. Backhaus-Ricoult, K. Burger and W. Mader: Ceramic Microstructures '86, ed. by J. A. Pask and A. G. Evans, Plenum Press, New York, (1987), 295.
72) K. Burger: "Material Transport Mechanisms Acting in Solid-State Bonding of Nb to Alumina", Doctoral thesis

to University of Stuttgart, (1987).
73) B. Gibbesch, G. Elssner, W. Mader and H. Fischmeister: *Ceram. Eng. Sci. Proc.*, **10** (1989), 1503.
74) B. Gibbesch, G. Elssner, W. Mader and H. F. Fischmeister: Joining of Ceramics, Glass and Metal, ed. by W. Kraft, DGM, Oberursel, (1989), 65.
75) L. J. Bostelaar, G.J.A. Klumperman, A.J.C. v.d. Ven and J.F.M. Caers: Joining of Ceramics, Glass and Metal, ed. by W. Kraft, DGM, Oberursel, (1989), 273.
76) T. Suga, K. Miyazawa and Y. Yamagata: Proc. of MRS Int. Meeting on Advanced Materials, Vol. 8, Metal–Ceramic Joints, MRS, Pittsburgh, PA, (1989), 257.
77) D. L. Johnson: "New Method for Obtaining Volume", *J. Appl. Phys.*, **40** (1969), 192.
78) S. E. Elliot and M. F. Ashby: Mechanism Mapping of Sintering under an Applied Pressure, CUED/C-MATS/TR.38, Cambridge Univ. Engineering Dept., Cambridge U.K., (1977).
79) Y. Fukuzawa, G. Elssner, G. Petzow, Y. Aono, E. Kuramoto, Y. Ando, Y. Kato and H. Yamaki: Proc. of MRS Int. Meeting on Advanced Materials, Vol. 8, Metal–Ceramic Joints, MRS, Pittsburgh, PA, (1989), 239.
80) K. Suganuma, T. Okamoto and M. Koizumi: *J. Am. Ceram. Soc.*, **67** (1984), C-256.
81) K. Suganuma and T. Okamoto: Fundamentals of Diffusion Bonding, ed. by Y. Ishida, Elsevier, Amsterdam, (1987), 71.
82) F. Hatakeyama, K. Suganuma and T. Okamoto: *J. Mater. Sci.*, **21** (1986), 1030.
83) M. G. Nicholas and R. M. Crispin: *J. Mater. Sci.*, **17** (1982), 3347.
84) M. Turwitt, G. Elssner and G. Petzow: *Z. Zahnärztl. Implantol.*, **2** (1986), S38.
85) K. Burger, D. Brenner and G. Petzow: *Z. Zahnärztl. Implantol.*, **3** (1987), S47.
86) K. Burger, W. Schulte and G. Petzow: *Z. Zahnärztl. Implantol.*, **4** (1988), 22.
87) B. Gibbesch, G. Elssner and G. Petzow: *Int. J. Oral & Maxillofacial Implants*, **4** (1989), 131.
88) B. Gibbesch, G. Elssner, E. Bischoff and G. Petzow: *Z. Zahnärztl. Implantol.*, **5** (1989), 108.
89) T. Yamada, A. Kohno, K. Yokoi and S. Okada: Fundamentals of Diffusion Bonding, ed. by Y. Ishida, Elsevier, Amsterdam, (1987), 489.
90) M. Courbiere, D. Juve, D. Treheux, C. Beraud, C. Esnouf and G. Fantozzi: High Tech Ceramics, ed. by P. Vincenzini, Elsevier, Amsterdam, (1987), 1053.
91) M. Courbiere, D. Treheux, C. Beraud, C. Esnouf, G. Thollet and G. Fantozzi: *J. de Physique*, **47** (1986), C1-187.
92) Y. Arata, A. Ohmori, W. K. Wlosinski and S. Sano: *Trans. JWRI*, **17** (1988), No. 2, 73.
93) S. Piech, W. Wlosinski, A. Ohmori and Y. Arata: Joining of Ceramics, Glass and Metal, ed. by W. Kraft, DGM, Oberursel, (1989), 115.
94) J. A. Wasynczuk and M. Rühle: Ceramic Microstructures '86, ed. by J. A. Pask and A. G. Evans, Plenum Press, New York, (1987), 341.
95) K. P. Trumble and M. Rühle: The Role of Oxygen in Spinel Interphase Formation during Ni/Al_2O_3 Diffusion Bonding, to be published.
96) Y. Ito, H. Oba and M. Kanno: Joining of Ceramics, Glass and Metal, ed. by W. Kraft, DGM, Oberursel, (1989), 205.
97) N. Iwamoto and Y. Makino: *Ceram. Eng. Sci. Proc.*, **10** (1989), 1745.
98) N. James and B. Derby: Joining of Ceramics, Glass and Metal, ed. by W. Kraft, DGM, Oberursel, (1989), 73.
99) Y. Fukuzawa, Y. Kojima, H. Aoshima and T. Kamata: Joining of Ceramics, Glass and Metal, ed. by W. Kraft, DGM, Oberursel, (1989), 139.
100) K. Atarashiya and Y. Hatanaka: Joining of Ceramics, Glass and Metal, ed. by W. Kraft, DGM, Oberursel, (1989), 199.
101) M. E. Brito, H. Yokoyama, Y. Hirotsu and Y. Mutoh: Proc. of MRS Int. Meeting on Advanced Materials, Vol. 8, Metal–Ceramic Joints, MRS, Pittsburgh, PA, (1989), 23.
102) M. E. Brito, H. Yokoyama, Y. Hirotsu and Y. Mutoh: *ISIJ Int.*, **29** (1989), 253.
103) Y. Iino and N. Tagushi: *J. Mater. Sci. Lett.*, **4** (1988), 981.
104) K. Kurokawa and R. Nagasaki: Proc. of MRS Int. Meeting on Advanced Materials, Vol. 8, Metal–Ceramic Joints, MRS, Pittsburgh, PA, (1989), 17.
105) K. Miura, T. Narita and T. Ishikawa: Proc. of MRS Int. Meeting on Advanced Materials, Vol. 8, Metal–Ceramic Joints, MRS, Pittsburgh, PA, (1989), 29.
106) M. Courbiere, M. Kinoshita and I. Kondoh: Joining of Ceramics, Glass and Metal, ed. by W. Kraft, DGM, Oberursel, (1989), 95.
107) K. Suganuma, T. Okamoto, M. Koizumi and M. Shimada: *J. Am. Ceram. Soc.*, **68** (1985), C-334.
108) Y. Aono, Y. Fukuzawa, Y. Ando, Y. Kato, H. Yamaki, K. Iwafuchi, T. Muroga, N. Yoshida and E. Kuramoto: Proc. of MRS Int. Meeting on Advanced Materials, Vol. 8, Metal–Ceramic Joints, MRS, Pittsburgh, PA, (1989), 245.
109) S. K. Choi, L. Froyen and M. J. Brabers: Joining of Ceramics, Glass and Metal, ed. by W. Kraft, DGM, Oberursel, (1989), 297.
110) R.C.J. Schiepers, F.J.J. van Loo and G. de With: *J. Am. Ceram. Soc.*, **71** (1988), C-284.
111) S. Morozumi, M. Endo, M. Kikuchi and K. Hamajima: *J. Mater. Sci.*, **20** (1985), 3976.
112) M. E. Brito, J. Matsumoto, Y. Hirotsu, Y. Fukuzawa and K. Tanaka: Joining of Ceramics, Glass and Metal, ed. by W. Kraft, DGM, Oberursel, (1989), 305.
113) M. Naka, T. Saito and I. Okamoto: *Trans. JWRI*, **17** (1988), No. 2, 67.
114) O. Ohashi: Proc. of MRS Int. Meeting on Advanced Materials, Vol. 8, Metal–Ceramic Joints, MRS, Pittsburgh, PA, (1989), 203.